

# LATE PLEISTOCENE-HOLOCENE CALDERA-FORMING EXPLOSIVE VOLCANISM OF THE GREAT KURIL ARC

S.Z. Smirnov<sup>1,✉</sup>, A.A. Kotov<sup>2</sup>, O.V. Bergal-Kuvikas<sup>3,4</sup>, A.V. Degterev<sup>5</sup>

<sup>1</sup>*V.S. Sobolev Institute of Geology and Mineralogy, Siberian Branch, Russian Academy of Sciences, pr. Akademika Koptyuga 3, Novosibirsk, 630090, Novosibirsk, Russia*

<sup>2</sup>*Tohoku University, Sendai, Katahira 2-1-1, Miyagi, 980-8577, Japan*

<sup>3</sup>*Institute of Volcanology and Seismology, Far Eastern Branch, Russian Academy of Sciences, Piip blv. 9, Petropavlovsk-Kamchatsky, 683006, Russia*

<sup>4</sup>*Vitus Bering Kamchatka State University, ul. Pogranichnaya 4, Petropavlovsk-Kamchatsky, 683032, Russia*

<sup>5</sup>*Institute of Marine Geology and Geophysics, Far Eastern Branch, Russian Academy of Sciences, ul. Nauki 1b, Yuzhno-Sakhalinsk, 693022, Russia*

Received: 1 October 2024

Accepted: 14 January 2025

Published online: April 2025

DOI: 10.2113/RGG20254817

## Citation:

**Smirnov S.Z., Kotov A.A., Bergal-Kuvikas O.V., Degterev A.V. (2025).**

Late Pleistocene-Holocene caldera-forming explosive volcanism of the Great Kuril Arc // *Russian Geology and Geophysics*, DOI: 10.2113/RGG20254817.

© S.Z. Smirnov, A.A. Kotov, O.V. Bergal-Kuvikas, A.V. Degterev, 2025

✉ *E-mail:* ssmr@igm.nsc.ru

Caldera-forming explosive volcanism is the most dangerous natural hazard, which has catastrophic consequences to the life, humans and their economic activities. The paper presents a summary of published and original data on the late Pleistocene-Holocene caldera-forming volcanism within the Great Kuril Arc (GKA) available to the recent times. The published data reveal that formation of explosive calderas occurred throughout all GKA segments in the late Pleistocene and Holocene. Most frequent it was in the Southern and Central segments of GKA, where it meets the back arc Kuril Basin. The majority of the studied calderas appeared in the late Pleistocene 50–12 Ka and early Holocene 8–6 Ka. Intensive caldera-forming volcanism in GKA could be contemporaneous to similar events in the East-Kamchatka Volcanic Belt and Southern Kamchatka. Caldera eruptions of GKA in the late Pleistocene and early Holocene were linked to evolution of large reservoirs of predominantly dacitic magmas, which were generated by partial melting of metabasitic protholiths in the shallow crust (3–12 km) at 810–930°C. Rhyolitic melts of these magmas were saturated with H<sub>2</sub>O, CO<sub>2</sub>, sulfur compounds, and probably other gaseous species. This caused shallow degassing at the pre-eruptive stages of the magma reservoir evolution. The study rises problems, which solution would provide a basis for effective prediction of catastrophic volcano explosions and monitoring of active GKA caldera volcanoes.

*Caldera, volcano, explosive volcanism, magmatism, Great Kuril Arc*

## INTRODUCTION

Explosive caldera-forming volcanism is believed to be one of the most dangerous natural phenomena with catastrophic consequences for wildlife, humans and their economic activities. It includes powerful explosive eruptions, accompanied by massive release of colossal amounts of magma (from the first tens to thousands of cubic km) and fragments of host rocks in the form of clastic avalanches, pyroclastic flows and tephra; from geological viewpoint they instantly (for hours or days) form thick pyroclastic deposits. Input of new magma do not compensate any more pressure drop due to rapid discharge of magma chamber. As a result, the roof and/or walls collapse inside the emptied space and a large depression appears at the earth's surface (Fig. 1). These depressions are commonly referred to as explosive calderas. They are contrasted with effusive calderas, which formation are not related to explosions. Instead, it occurs due to a lateral magma migration from the reservoir [Cole et al., 2005]. The term 'caldera' has been actively debated for a long time. By the present time, researchers, who study this type of volcanism, accept the definition given by H. Williams [Williams, 1941], who defined cal-

deras as large collapse depressions, more or less circular or cirque-like in form, the diameter of which is many times greater than any included vent [Leonov and Grib, 2004; Cole et al., 2005]. However, this definition leaves the problem of the difference between caldera and large crater unresolved. The boundary between them is recognized as conditional and by different researchers is regarded by the lesser depression diameter, which varies from about 1.6 to 2.5 km [Leonov and Grib, 2004].

The explosive calderas are concentrated predominantly within the Pacific 'Ring of Fire'. The Kuril-Kamchatka Island Arc System is a part of it, including the Great Kuril Arc (GKA), a chain of volcanic islands, stretching for 1200 km from the Kamchatka Peninsula, to the northern margin of Hokkaido Island (Japan).

The development of the Russian Far Eastern regions requires continuous operation of transport network, ensuring rapid economic growth, and exploration of natural resources. However, the active Kuril-Kamchatka Island Arc System poses a threat of natural hazard on the islands and unfavorable conditions for economic activity across the Far Eastern region. In its northern part, in the Kamchatka Peninsula, volcanic processes and phenomena are the subject of extensive multidisciplinary studies,



**Fig. 1.** Examples of the Great Kuril Arc calderas: *a* – the Golovnin Caldera (Kunashir Island); *b* – the Lvinaya Past Caldera (Iturup Island) (photo by I.A. Kirillova); *c* – the Zavaritsky Caldera Complex (Simushir Island) (photo by T.A. Kotenko); *d* – the Tao-Rusyr Caldera (Onkotan Island).

volcanic and seismic activity is monitored using modern instruments and methodology. The Holocene volcanism of Kamchatka has been studied in sufficient detail, the activity history of most eruptive volcanoes has been deciphered, including those volcanoes which contain large collapse calderas in their edifices (hereinafter we will call them *caldera volcanoes*). The Kuril Islands are much worse studied in this regard: after systematic geological and geophysical work at the beginning of the second half of the 20th century, the research activity has sharply reduced. In subsequent years, despite rapid development of geochemical and geochronological methodology, the geological investigations were extremely limited and carried out not systematically. It should be noted that the most powerful eruptions with the caldera collapses occurred in the nearest geological past in the southern, most populated and economically developed part of the island archipelago. This is not far from economic centers of the Russian Far East – Petropavlovsk-Kamchatsky and Yuzhno-Sakhalinsk, as well as Vanino transportation hub. Vladivostok, Nikolaevsk-on-Amur, Komsomolsk-on-Amur are located at a distance of 1000–1100 km from

GKA caldera volcanoes. They may also suffer from ash-falls produced by the most powerful ( $VEI \geq 5$ ) eruptive events. Air transportation routes connecting the countries of Southeast Asia with North America and various regions of the Russian Far East run to the east and west in vicinity of the Kuril Islands. Even moderately strong explosive eruptions interfere with air traffic, while powerful caldera-forming events can completely stop it. This confirms the relevance of comprehensive study of the Kuril Island Arc caldera volcanism.

Despite the high risk of catastrophic events, the Quaternary caldera-forming volcanism in the Kuril Islands and related phenomena were among the least covered by scientific research and the attention of scientists. The purpose of this work is to systematize and summarize the data published in different years on the Quaternary caldera-forming volcanism of the Kuril Island Arc, supplementing them with our scientific results obtained recently, as well as to demonstrate to the scientific community the scale and relevance of the catastrophic explosive volcanism related problems in the region.

#### HISTORY OF STUDY OF CALDERA VOLCANISM OF THE GREAT KURIL ARC

In the late 18th century, the Russian government sent to the Kuril Islands the first volcanologic expedition to document the impact of 1778 explosive eruption of Raikoke Volcano, which claimed the lives of 15 Russian fur traders [Gorshkov, 1967]. The first volcanological survey of the entire Kuril Island chain was conducted 100 years later by a British volcanologist J. Milne [1878] during his service for the Japanese Empire [Milne, 1879]. Systematic studies of the Kuril volcanoes began in 1946, after the Kuril Islands returned under the USSR control [Gorshkov, 1958; 1967]. During these years, the volcanoes were described in general [Korsunskaya, 1956; Markhinin, 1959; Gorshkov, 1960; Ostapenko, 1970] and in some cases – the products of their eruptions as well [Gorshkov, 1961; Ostapenko et al., 1967].

Following the works by G.S. Gorshkov [1958, 1960], the next comprehensive description of the Kuril volcanoes was given by [Erlich, 1986]. This work contains information about 27 calderas, but the author admitted that original data were taken from the early catalogues, such as [Gorshkov, 1958]. Following these publications, a description of active caldera volcanoes of the Kuril Islands appeared in [Newhall and Dzurizin, 1988], which provided characteristics of only 11 calderas. These researchers also based mostly on the previous works of G.S. Gorshkov and E.N. Ehrlich. The most recent review on the Kuril Islands volcanoes, including caldera volcanoes, is presented in [Laverov, 2005]. Extensive studies of the Kuril caldera volcanoes, as it will be shown below, were conducted at the end of the 20th century. They were predominantly focused on the geothermal energy sources. The works of [Erlich and Meleseshev, 1974; Fedorchenko

et al., 1989] summarized the key results on felsic volcanism, including temporal distribution of eruptive activity in the Kuril Islands, deep structure beneath the centers of felsic volcanism, chemistry and petrogenesis of magmas involved. However, the region's inaccessibility and sparse population have hindered comprehensive studies of active volcanism in the GKA. Consequently, fundamental aspects of volcanic history, tectonic controls, and deep magmatic processes associated with caldera-forming eruptions remain poorly constrained. These research gaps were further aggravated by the political and economic challenges faced by the country during the late 20th and early 21st centuries.

### AGE AND DISTRIBUTION OF THE QUATERNARY CALDERAS OF THE KURIL ISLANDS

As evidenced by historical review, different researchers have identified between 11 and 27 calderas within the GKA. The latest published reviews on Kuril volcanoes [Bazanova et al., 2016; Laverov, 2005] demonstrate that single or nested calderas are the main morphostructural elements in 21 volcanoes on the Kuril Islands. Fig. 2–4 show 18 volcanoes where calderas are clearly expressed in the topography and/or their presence confirmed by an appropriate pyroclastic deposits. A summary on these calderas is provided in the Electronic Appendix, Table S1.

Traditionally, GKA is divided into three segments: the Northern, which includes the islands between the First Kuril Strait and the Kruzenshtern Strait; the Central – between the Kruzenshtern and Bussol straits and the Southern – between the Bussol and Izmeny straits [Gorshkov, 1967; Fedorchenko et al., 1989].

The Quaternary caldera volcanoes were identified in all GKA segments, but they are unevenly distributed. They are most abundant in the Southern segment (Fig. 2). Here, seven calderas are clearly expressed on Kunashir Island (Mendelev and Golovnin calderas) (Fig. 1a) and Iturup Island (Lvinaya Past (Fig. 1b), Urbich, Tsirk, Kamui, Medvezhya). According to [Bazanova et al., 2016], the Medvezhiya caldera (10 × 9.5 km) is the largest subaerial caldera of GKA. Iturup Island is the absolute leader among the GKA islands in the number of subaerial Quaternary calderas. A similar large submarine object is the Gorshkov Caldera (9-p6.11 according to [Avdeiko et al., 1992]), discovered in the area of the Chyornye Bratya Islands. According to [Bazanova et al., 2016], its diameter is 14 × 11 km. However, the study of Kuril Island Arc submarine volcanoes indicates in this place two nested calderas 15 × 20 and 7.5 × 11.5 km [Avdeiko et al., 1992; Bondarenko and Rashidov, 2003]. A large submarine caldera (15 × 9 km) supposedly is associated with Broughton Island [Bazanova et al., 2016; Laverov, 2005].

The oldest dated GKA caldera is the Medvezhiya Caldera on Iturup Island,  $0.41 \pm 0.1$  Ma [Ermakov and Stein-

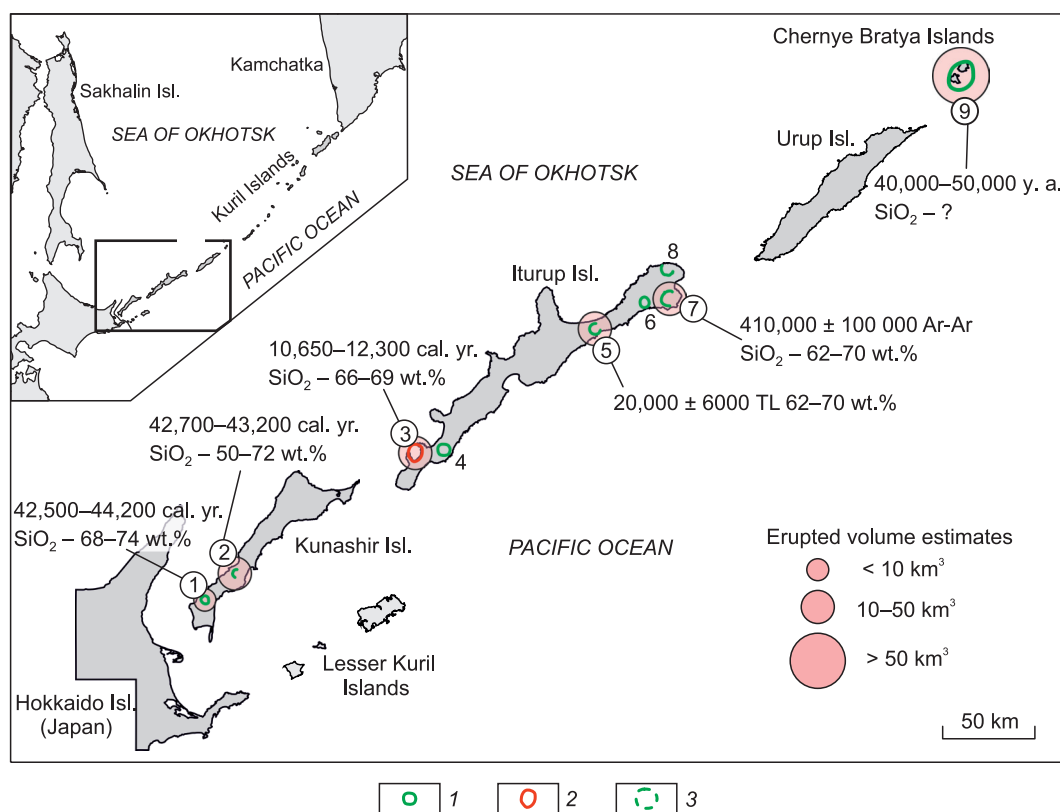


**Fig. 2.** Calderas of the GKA Southern segment. Calderas: 1 – Pleistocene, 2 – Holocene, 3 – supposed. Caldera numbers correspond to those in Table S1, Supplementary materials.

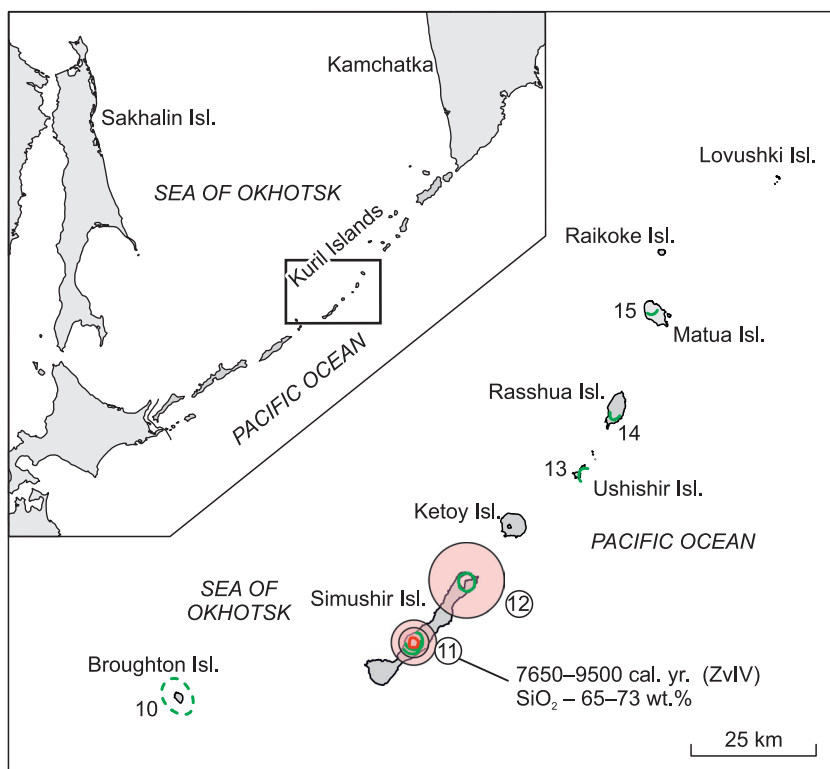


Fig. 3. Calderas of the Central GKA segment. The symbols are the same as in Fig. 2.

berg, 1999], (Ar-Ar). All other ages of such eruptions date back to the end of the late Pleistocene (41–12.4 ( $^{14}\text{C}$ ) Ka).

Outcrops of pumice tuffs reaching about 264 m in thickness are known to the west of the Vetrovoy Isthmus on Iturup Island [Laverov, 2005; Smirnov et al., 2019]. These rocks have been formed between  $38,500 \pm 500$  and  $5,350 \pm 50$  y.a. ( $^{14}\text{C}$  dating, after [Bulgakov, 2018]) or  $42,400 \pm 700$  and  $6,120 \pm 80$  cal. y.a., respectively (hereinafter we give the values of the calendar age (cal. y.a.) obtained by calibrating the radiocarbon age according to [Bronk Ramsey, 1995] using OxCal v. 4.4.4 software (c14.arch.ox.ac.uk/oxcal.html) More accurate radiocarbon dates of the eruption are not available. According to thermoluminescence dating, the eruption occurred  $20,000 \pm 6,000$  y.a. [Bulgakov, 2018]. With an estimated eruptive volume ( $\sim 100 \text{ km}^3$ , after [Melekestsev et al., 1988]), these pyroclastic deposits correspond to the event, which is comparable in magnitude to the most powerful explosive eruptions of the Kuril-Kamchatka Volcanic System. Recent finding of a dacitic pumice layer of  $2,056 \pm 60$  and  $2,064 \pm 237$  cal. y. a. [Bergal-Kuvikas et al., 2023] confirms the late Holocene activity of this volcanic center.

Caldera of Lvinaya Past Volcano on Iturup Island is one of the youngest in the Southern segment. According to [Melekestsev, 1974; Braitseva et al., 1995] it was formed in the Holocene  $9,400^{14}\text{C}$  y.a. ( $10,650$  cal. y.a.). The recent data by [Degterev et al., 2015], however, provides more ancient ages –  $12,260 \pm 220$  and  $12,360 \pm 170$  cal. y. a., corresponding to the end of the late Pleistocene.

While the land area in the Central segment of GKA is substantially smaller than the Southern segment (Fig. 3), both regions host comparable number of caldera volcanoes. There are three subaerial calderas and 1 caldera complex in Simushir, Rashua and Matua islands. The largest of them are the calderas of Simushir Island with diameters of about 6–7 km (Fig. 1c). A large submarine caldera is supposed to exist in the area of Ushishir Islands  $8 \times 6$  km by [Laverov, 2005; Bazanova et al., 2016] or  $\sim 5$  km by [Bondarenko and Rashidov, 2018]. It is suggested that the Central segment concentrates the maximum volume of erupted rocks when compared to other GKA segments [Bergal-Kuvikas, 2015].

There are very few absolute dates on caldera-forming eruptions in the Central GKA segment. According to geomorphological evidence, most of them likely formed during the late Pleistocene [Melekestsev, 1974; Bazanova et al., 2016]. The Zavaritsky IV Caldera eruption on Simushir Island has been assigned a Holocene age based on its geomorphological features [Bazanova et al., 2016]. This estimate is consistent with ages obtained for tephra from this eruption defined in distal soil profiles, which range between  $8.5$  and  $6.8$   $^{14}\text{C}$  Ka ( $9,500$ – $7,650$  cal. y.a.) [Nakagawa et al., 2008; Dirksen and Rybin, 2020]. The Matua caldera of  $3.5 \times 5$  km size was formed at the end of late Pleistocene, about  $11,500$ – $12,000$  y.a., by a partial collapse of the pre-caldera volcanic edifice [Degterev et al., 2012; Rybin et al., 2017].

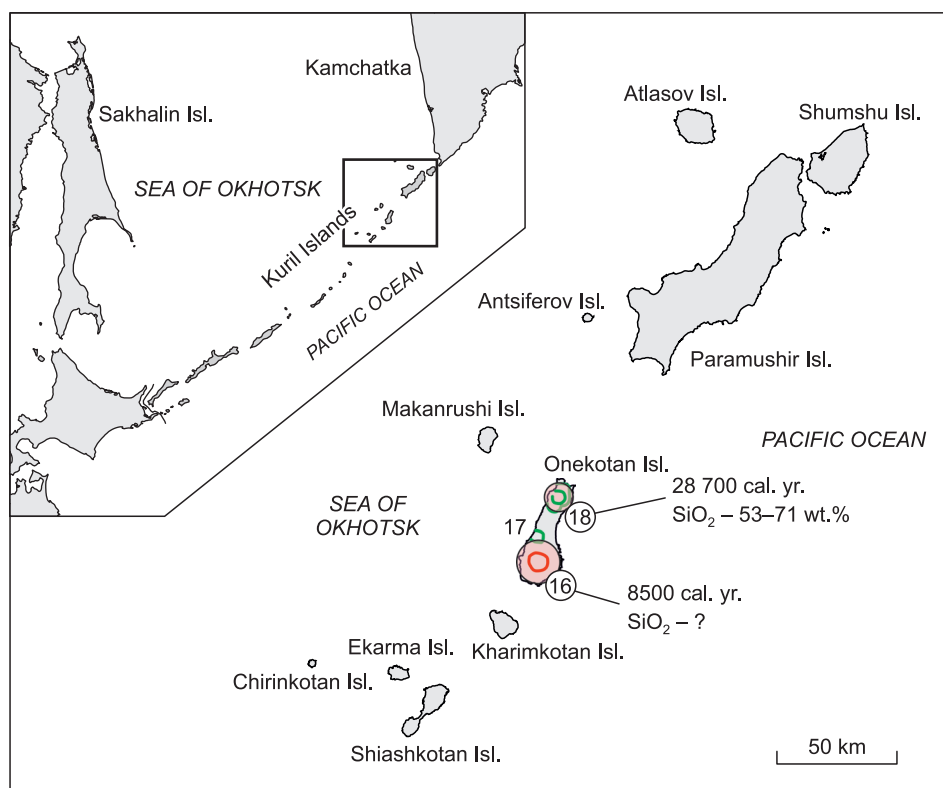


Fig. 4. Calderas of the Northern GKA sector. The symbols are the same as in Fig. 2.

The Northern GKA segment (Fig. 4) differs from the Southern and Central by the smallest number of late Pleistocene-Holocene calderas. They represent the main centers of the Quaternary volcanism on Onekotan Island. Judging by geomorphology, the most ancient of them is the Kryzhanovsky Caldera, which is no older than the late Pleistocene [Laverov, 2005]. The latest caldera-forming eruption of the Nemo caldera complex, called Nemo III, occurred at  $24,500\text{--}25,000^{14}\text{C Ka}$  ( $28,700 \pm 600$  cal. y.a.) [Melekestsev et al., 1997]. The youngest event on Onekotan is associated with the island's largest volcanic center – the Tao-Rusyr Caldera (Fig. 1d),  $7,500 \pm 80^{14}\text{C y. a.}$  ( $8,400$  cal. y.a.) [Melekestsev et al., 1974; Braitseva et al., 1995].

Several publications declare calderas at multiple Kuril sites – including Ketoy Island, the Grozny Ridge, Atsonupuri Volcano, Chirip Peninsula's volcano-tectonic depression (Iturup), Kuntomintar and Sinarka (Shiashkotan), Kharimkotan Island, and Tyatya Volcano (Kunashir) [Erlich, 1986; Rybin et al., 2015]. We do not discuss them here because of their small sizes or because many identifications remain morphologically or geologically unsubstantiated.

## GEOLOGY OF CALDERAS

Detailed data on the structure and geologic setting of Pleistocene and Holocene calderas on GKA islands are much sparser than for the Eastern and Southern Kam-

chatka calderas. Currently, the most comprehensive information, including detailed geological maps and diagrams, as well as description of pyroclastic deposits, is available for only two of them: the Nemo Caldera (Onekotan Island) [Melekestsev et al., 1997] and the Medvezhiya Caldera (Iturup Island) [Ostapenko, 1970; Ermakov and Semakin, 1996; Ermakov and Steinberg, 1999]. However, scientific interest in the Medvezhiya Caldera stems less from its formation mechanisms than from its post-caldera evolution, particularly linked to the ore mineralization within Kudryavy Volcano's crater and the occurrence of high-Mg basalts [Marynov et al., 2023; Kuzmin et al., 2023].

The geologic architecture of caldera volcanoes typically comprises three principal elements: (1) pre-caldera basement formations, (2) syn-caldera morphostructures and deposits, and (3) post-caldera volcanic formations.

According to the position of relatively earlier volcanic edifices (pre-caldera formations), the collapse calderas related to eruption of intermediate and felsic magmas is divided into those confined to the preceding volcanic edifice or structure (Group B<sup>1</sup>) and those cutting different

<sup>1</sup> Calderas are classified after [Leonov and Grib, 2004]: Group A – calderas of basalt volcanoes, Groups B–D – calderas of volcanoes of intermediate and felsic composition: B (in original Cyrillic version Б) – confined to one volcanic structure, C (in original Cyrillic version В) – cutting several volcanic edifices, D (in original Cyrillic version Г) – calderas in areas where volcanism was absent or insignificant at the pre-caldera stages.

pre-existing volcanic structures (Group C) [Erlich, 1986; Leonov and Grib, 2004].

The vast majority of GKA calderas belong to Group B. They exclusively develop atop large single shield volcanoes and stratovolcanoes, which represent pre-caldera basement formations. The most prominent example of these calderas is the Tao-Rusyr Caldera (Onekotan). Group C includes large calderas, e.g. Medvezhiya (Iturup), Mendeleev (Kunashir), Nemo (Onekotan). Typically, they develop on erosion surfaces of the Neogene to Quaternary volcanic edifices. In both cases, caldera formation may be separated from preceding volcanism by prolonged hiatus periods. For the Nemo Caldera complex, this period is estimated at ~ of 650 Ka [Melekestsev et al., 1997]. Comparable temporal gap (~ 600 Ka) supposedly separates the last lava flows of pre-caldera shield volcano and Medvezhiya Caldera formation [Ermakov and Steinberg, 1999]. Golovnin Caldera on Kunashir Island is probably another representative of Group C calderas.

The Vetrovoy Isthmus (Iturup) holds a unique position among the centers of caldera-forming eruptions in GKA. Current interpretations suggest that the eruption producing thick pumice deposits in this area occurred within the coastal paleoenvironment of the late Pleistocene shallow marine strait, which separated ancestral islands corresponding to the present-day Grozny Range and the Medvezhiy Peninsula [Afanasev et al., 2020]. Volcanic edifices that can be attributed to the pre-caldera stage, according to [Kovtunovich et al., 2002], presumably have Pliocene-Pleistocene ages. Thus, significant temporal gap separates them from the pyroclastic deposits. The absence of distinct morphological features of caldera, e.g. circular scarps, rounded or oval depression, etc., despite a sufficiently large erupted volume, represents an anomalous characteristic of this volcanic formation. This is why the position of the eruptive center has not been located yet. Various researchers place it either in the center of the Vetrovoy Isthmus [Gorshkov, 1967], or into the Prostor Bay [Avdeiko et al., 1992; Laverov, 2005].

Available data indicate that both single calderas and complexes including several nested calderas exist on GKA islands. Examples of single calderas include the Golovnin (Kunashir), Tao-Rusyr (Onekotan), Broughton (Simushir) calderas. The complexes of the Nemo (Nemo I, Nemo II and Nemo III) and Zavaritsky (Zavaritsky I, Zavaritsky II, Zavaritsky III, Zavaritsky IV) volcanoes exemplify the nested calderas [Laverov, 2005; Bazanova et al., 2016]. Seismoacoustic and stratigraphic data show that Lvinaya Past Volcano on Iturup Island also consists of two nested calderas [Bondarenko, 1991; Degterev et al., 2015].

During major explosive island eruptions, the majority of pyroclastic material is deposited into marine environments, while terrestrial preservation tends to be fragmentary and highly susceptible to erosion [Melekesysev et al., 1997]. Caldera-forming eruptions generate eruptive material comprising both proximal deposits (including mas-

sive tuff and ignimbrite sequences, debris avalanche deposits, and ballistic ejecta) and distal tephra deposits, the latter typically constituting a substantial proportion of the total erupted volume. Thick proximal deposits are known from Golovnin, Mendeleev, Lvinaya Past, Medvezhiya, and Nemo III calderas. The thicknesses of proximal deposits can reach several tens or even hundreds of meters. For example, in the Vetrovoy Isthmus (Iturup), the tuff thickness reaches maximum elevations of about 260 m, while their base remains below sea level.

Distal tephra from caldera eruptions can cover vast areas exceeding tens and hundreds of millions of square kilometers, creating widespread tephrostratigraphic marker horizons both in terrestrial and marine sedimentary records [Ponomareva et al., 2015]. However, for GKA calderas, documented tephra findings in terrestrial soils and deep-sea drilling cores remain limited to isolated occurrences.

The distal tephra, compositionally similar to eruptive products of the Zavaritsky Caldera (Simushir Island), has been identified both in marine sediments from the central Sea of Okhotsk [Derkachev et al., 2016] and terrestrial soil deposits on the islands to the north of Simushir [Dirksen and Rybin, 2018, 2020; Nakagawa et al., 2008]. This demonstrates tephra dispersal over a distance up to 700 km from the source. This tephra was supposedly also found on Kamchatka [Dirksen and Rybin, 2020]. Distal tephra of a major (VEI 4–5) eruption near Vetrovoy Isthmus (~2,000 y.a.) has been identified in the soil deposits across the islands of the Southern and Central segments of the archipelago [Bergal-Kuvikas et al., 2023]. This tephra forms the distinctive CKr marker horizon, demonstrating a dispersal range extending up to 400 km from its eruptive source [Nakagawa et al., 2008]. The Nemo Caldera tephra has been found in marine sediments of the Sea of Okhotsk [Derkachev and Portnyagin, 2013]. Deep-sea drilling cores both from the Sea of Okhotsk and in the Detroit seamount (Emperor Seamount Chain, NW Pacific) contain ashes presumably related to the other Kuril Island Arc volcanoes [Ponomareva et al., 2023].

Extrusive domes formed by eruption of residual degassed magma typically localized along ring faults, may also belong to the syncaldera stage. The Mendeleev Caldera exemplifies this process with more than 20 syncaldera domes extruding through its pumiceous pyroclastic deposits [Kotov et al., 2023]. However, understanding of extrusive syncaldera volcanism across the Kuril Island Arc remains fragmentary and requires further detailed geologic studies.

Post-caldera volcanism characterizes nearly all considered eruptive centers, with notable exceptions of the Lvinaya Past, Urbich and Tsirk calderas on Iturup Island. Following Leonov and Grib [2004] we consider the nested caldera formation as a part of the caldera-forming stage. However, the final caldera (IV) formation at Zavaritsky Volcano (Simushir Island) resulted from the collapse of a post-caldera edifice [Laverov, 2005]. Most

GKA post-caldera volcanoes developed during the late Pleistocene to Holocene (Electronic Appendix, Table S1), with many remaining active today.

Post-caldera volcanic activity manifests through the formation of stratovolcanoes and extrusive domes. All of them are confined either in the intracaldera depressions or along the caldera rim structures. In the Medvezhiya and Gorshkov calderas, this activity has produced complex volcanic edifices that form mountain ranges within the caldera depressions. The relatively small calderas on Rasshua and Matua islands are barely distinguished in the island topography due to being largely obscured by the post-caldera edifices of Rasshua and Peak Sarychev volcanoes.

### MAGMA CHEMISTRY AND MAGMA STORAGE CONDITIONS

Currently, it is a common knowledge that large-volume caldera-forming eruptions typically originate from reservoirs containing highly evolved, volatile-rich silicic magmas with elevated viscosity [Bachmann and Bergantz, 2008]. The scales of caldera eruptions presume that these reservoirs might contain from first to several thousand cubic kilometers of such magmas. Consequently, pre-eruptive magmatic processes preceding caldera formation should operate at substantial spatial and temporal scales.

Compared to the geologic structure and eruptive chronology of GKA calderas, their magma storage characteristics and petrogenetic evolution remain significantly understudied. In their first review Erlich and Melekestsev [1973] proposed, based on petrochemical evidence, that felsic magmas in GKA calderas separate directly from parental mantle-derived magmas at depths exceeding 15 km, thus excluding the crustal partial melting, as a possible generation mechanism. This view has not been questioned for a long time, since petrological and geophysical studies of GKA were limited. Advanced analytical techniques developed over past two decades yielded new data inspiring a comprehensive reassessment of felsic magma petrogenesis at the GKA.

The whole rock pumice and ignimbrite compositions from the late Pleistocene–Holocene GKA caldera-forming eruptions and electron-microprobe analyses (EMPA) of their groundmass glasses are compiled in Electronic Appendix, Tables S2 and S3. Currently, comprehensive petrographic and geochemical data for the products of GKA caldera-forming eruptions are available only for a limited number of volcanic centers, notably the Mendeleev Caldera [Kotov et al., 2023], the Lvinaya Past [Ostapenko et al., 1967; Smirnov et al., 2017], the Vetrovoy Isthmus [Ostapenko, 1967; Smirnov et al., 2019], the Medvezhiya Caldera [Ostapenko, 1970; Ostapenko et al., 1967; Marynov et al., 2023], the Zavaritsky Caldera [Ostapenko et al., 1967] and the Nemo III Caldera [Melekestsev et al., 1997].

Deposits of caldera-forming eruptions are represented by ignimbrites, as well as pumice, lapilli and ash tuffs. Foreign researchers usually call any deposits of pumice pyroclastic flows as ignimbrites, regardless of the degree of their welding [Sparks et al., 1973; Giordano and Cas, 2021], thus giving the term a genetic sense. Nevertheless, in this paper we will adhere to the division of pyroclastic rocks into tuffs, which are characterized by a low welding degree, and ignimbrites – welded pyroclastic rocks with fiamme structures [Luchitsky, 1971], giving the term a more petrographic meaning. Ignimbrites are found in sections of proximal pyroclastic deposits of the Medvezhiya, Zavaritsky and Nemo III calderas [Ostapenko, 1970; Ostapenko et al., 1967; Ermakov and Steinberg, 1999; Melekestsev et al., 1997]. Pumice tuffs are present in all pyroclastic deposits without exception. Relationship to caldera formation of intracaldera deposits of rhyolitic pumice associated with the Menshiy Brat post-caldera volcano in the Medvezhiya Caldera is uncertain. However, since they are texturally, structurally and geochemically close to pumice of caldera eruptions from other GKA volcanoes, we will consider them together.

Fig. 5, 6 show whole-rock compositions of pumices and ignimbrites from the Quaternary caldera-forming eruptions in the GKA. We consider that pumice compositions are better proxy for a magma chemistry, unlike ignimbrites, which often contain a mixture of magmatic (juvenile) and clastic (resurgent) components. The presented rocks exhibit a broad range from basalts to rhyolites, with dacitic and rhyodacitic compositions predominating (average  $\text{SiO}_2 = 67$  wt. %). Ignimbrites consistently show the lower silica contents, while pumices are more silicic. The highest silica contents, according to available data, occur in intracaldera pumices from Menshiy Brat Volcano (Fig. 5). Notably dacitic tuffs of Golovnin Caldera contain horizons of banded pumice featuring anorthite megacrystals and large olivine-anorthite intergrowths. These pumices correspond to basalts and basaltic andesites – the most mafic samples in the available dataset.

The ignimbrites and pumices from caldera eruptions shown in Fig. 5b correspond to low- and medium-K series and cluster near the magnesian-ferroan boundary in Fig. 5c. Samples from Iturup Island and the Nemo III Caldera (Onkotan) plot near the low/medium-K transition (average  $\text{K}_2\text{O} = 1.2$  wt.%), while those from the Kunashir Islands and Zavaritsky calderas (Simushir), exhibit low-K characteristics (average  $\text{K}_2\text{O} = 0.79$  wt.%). In all studied compositions sodium consistently dominates among the main alkali metals ( $\text{Na}_2\text{O}/\text{K}_2\text{O} > 2.4$ ).

The most pronounced variations appear in  $\text{Na}_2\text{O}$  and particularly  $\text{K}_2\text{O}$  contents. Samples from Kunashir and Iturup islands display the lowest total alkali contents, plotting within low-alkalinity field (Fig. 5a). In contrast, ignimbrites of the Nemo III Caldera (Onkotan Island) contain slightly higher alkali concentrations, placing them in the lower portion of normal alkalinity field

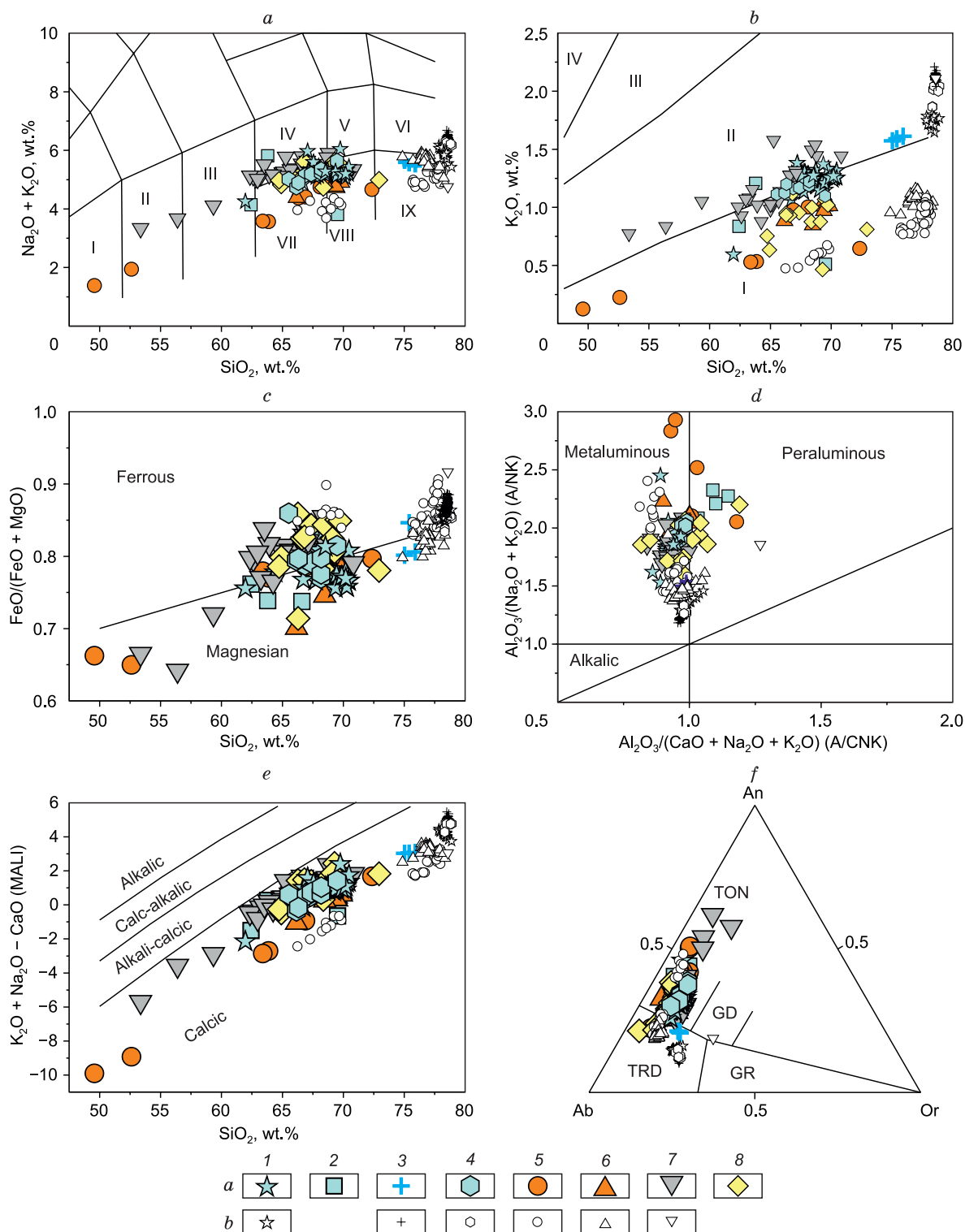


**Fig. 5.** Compositions of pumice and ignimbrites bulk rocks and groundmass glasses from GKA caldera eruptions (wt. %). Iturup Island: 1 – pumice of the Vetrovoy Isthmus; 2 – pumice and ignimbrites of the Medvezhiya Caldera; 3 – pumice of Menshiy Brat Volcano; 4 – pumice of the Lvinaya Past Caldera. Kunashir Island: 5 – pumice of the Golovnin Caldera; 6 – pumice of the Mendeleev Caldera. Onkotan Island: 7 – pumice and ignimbrites of the Nemo III Caldera. Simushir Island: 8 – pumice of the Holocene caldera eruption of the Zavaritsky Complex. *a* – whole rock compositions; *b* – groundmass glass compositions. Symbols: *a*: I – basalt, II – basaltic andesite, III – andesite, IV – dacite, V – rhyodacite, VI – rhyolite, VII – low-alkaline dacite, VIII – low-alkaline rhyodacite, IX – low-alkaline rhyolite; *b*: I – low-potassium series, II – medium-potassium series, III – high-potassium series, IV – ultra-potassium series; *f*: TON – tonalite, TRD – trondhjemite, GD – granodiorite, GR – granite. Classification diagrams, according to the Petrographic Code [2009] (*a*), Rickwood [1989] (*b*), Frost [2001] (*c*), Shand [1943] (*d*), Frost [2001] (*e*), Barker [1979] (*f*).

(Fig. 5a). Rocks from GKA caldera-forming eruptions are enriched with CaO (averaging ~ 4 wt.%) at normal and low total alkali contents, and therefore their compositions are classified as calcareous (Fig. 5e).

The vast majority of compositions fall within the metaluminous field or cluster near the metaluminous-peraluminous boundary, with an average A/CNK ratio of 0.95 (Fig. 5d). Only a minor part of ignimbrites and pumices

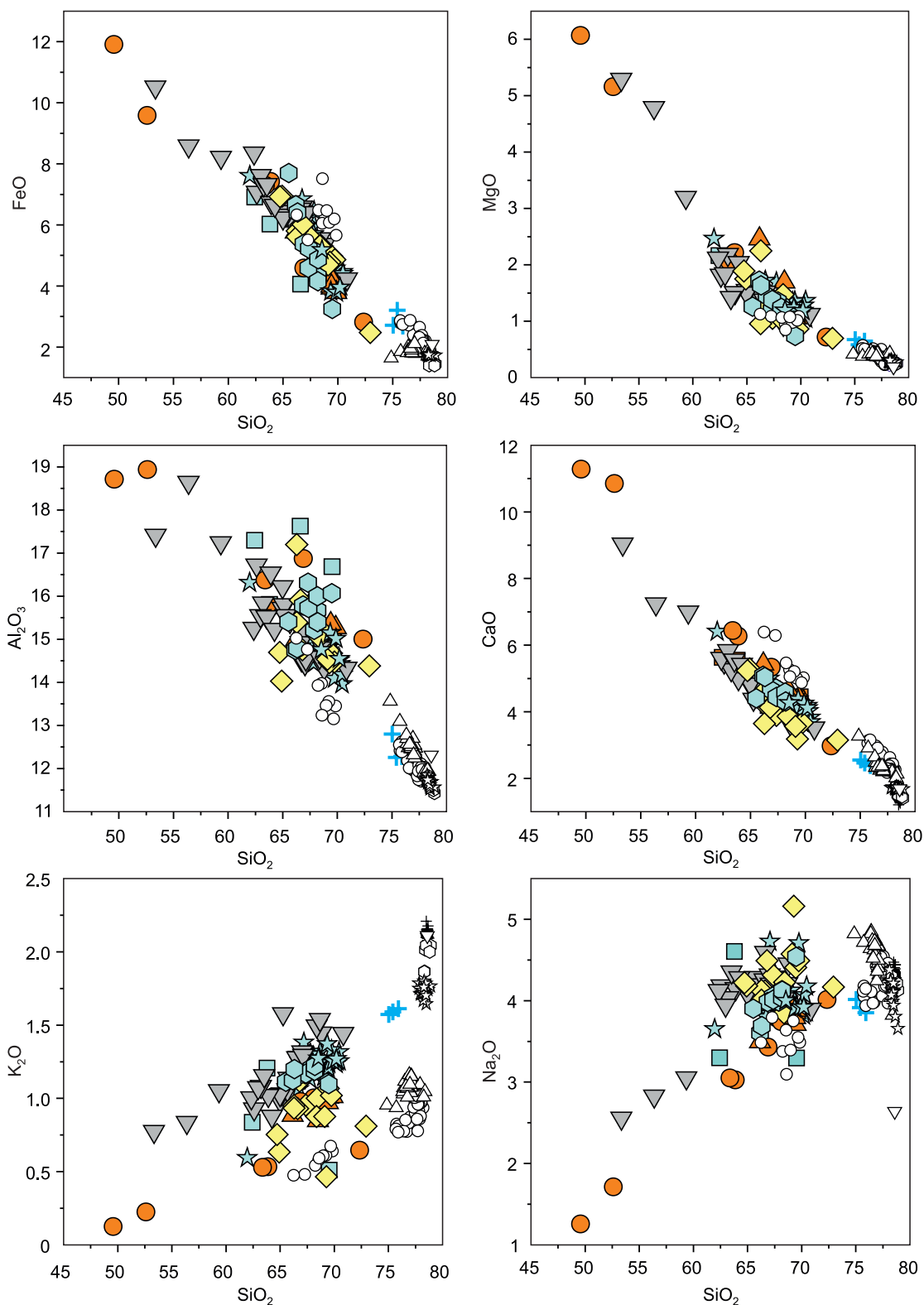


**Fig. 6.** Compositional variations of GKA caldera pumice and ignimbrite bulk rock and groundmass glass (wt. %). The symbols are the same as in Fig. 5.

from the Zavaritsky, Golovnin and Medvezhiya calderas exhibit peraluminous characteristics. As silica content increases, the products of caldera-forming eruptions (their compositions are shown in Fig. 6) are depleted in FeO, MgO, CaO, Al<sub>2</sub>O<sub>3</sub> and enriched in K<sub>2</sub>O, Na<sub>2</sub>O.

The chemical characteristics of ignimbrites and pumices described above demonstrate that juvenile material from caldera eruptions is compositionally similar to island-arc and ophiolitic plagiogranites. These rocks correspond to M-type granitoids [White, 1979] (Fig. 4f) that typically form through melting of metabasic crustal substrates.

The phenocryst assemblages in pumices consist predominantly of plagioclase (its composition varies over a wide range, An<sub>40–95</sub>), clinopyroxene (augite-diopside), orthopyroxene (hypersthene) and titanomagnetite. Ilmenite is present occasionally. Quartz occurs only in the most siliceous pumices. Amphibole phenocrysts – low-alumina magnesian hornblende, were found in pumices from the Lvinaya Past [Smirnov et al., 2017], the Matua (oral presentation by A.V. Rybin) and the Rashua [Gorshkov, 1967] calderas. Relics of high-alumina magnesian hornblende, tschermakite, and magnesiohastingsite were also identified within clino- and orthopyroxenes from the Vertovoy Isthmus (Iturup) [Smirnov et al., 2019] and the Mendeleev Caldera (Kunashir) pumices [Kotov et al., 2023].

Bulk compositions of volcanic rocks offer preliminary insight into magma chemistry. Pyroclastic rocks of explosive eruptions incorporate not only juvenile material but also xenoliths of rocks through which magma ascends to the surface, and clastic debris derived from fragmentation of the conduit walls and volcanic edifices. Analysis of fresh groundmass glass and phenocryst-hosted melt inclusions, which preserve direct records of melt compositions, are necessary for more precise constraints on magma chemistry.

Recent studies have provided new melt inclusion data from pumices of the late Pleistocene large caldera-forming eruptions across GKA islands. They include analyses from the Mendeleev (Kunashir Island) [Kotov et al., 2023], Lvinaya Past (Iturup Island) [Smirnov et al., 2017] calderas and dacitic pumice deposits in the Vetrovoy Isthmus (Iturup Island) [Smirnov et al., 2019]. Published groundmass glass compositions of caldera-forming eruption rocks remain limited, encompassing dacitic pumice from the Vetrovoy Isthmus and Lvinaya Past Volcano, as well as intracaldera rhyolite pumice of the Medvezhiya Caldera [Bergal-Kuvikas et al., 2023]. Individual groundmass glass analyses are also available for eruptive rocks from Nemo III, Golovnin and Mendeleev calderas [Melekestsev et al., 1997; Razzhigaeva et al., 2016].

Compositional data for naturally quenched vitreous melt inclusions in pumice minerals of caldera eruptions of the Southern GKA segment are summarized in the Electronic Appendix, Table S4. Despite rapid quenching conditions, melt inclusion glasses may exhibit compositional deviations from the parental melts due to post-en-

trapment crystallization onto inclusion walls. Fig. 7, 8 demonstrate significant compositional overlap between groundmass and melt inclusion glasses, indicating consistency between these two melt proxies. This suggests minimal impact of post-entrapment crystallization on compositions of melt inclusions, supporting their representability for the mineral-forming melt chemistry (detailed description of methodologies are presented in [Smirnov et al., 2017; 2019; Kotov et al., 2021; 2023]). At the same time, compositions of melt inclusions and groundmass glasses substantially differ from bulk rock compositions. In some cases, they belong to the evolutionary trend with bulk rock compositions, but more often fall aside. The K<sub>2</sub>O-SiO<sub>2</sub> diagram in Fig. 9 shows a comparison of groundmass glass compositions of the late Pleistocene-Holocene GKA caldera eruption pumice and ignimbrites with those from Hokkaido Island and ash particles from the Sea of Okhotsk sediments [Razzhigaeva et al., 2016; Derkachev et al., 2016].

With noticeable variations in pumice whole-rock compositions, the melt compositions of the Lvinaya Past Caldera, the Vetrovoy Isthmus and rhyolite pumice of Menshyi Brat Volcano (Medvezhiya Caldera) vary in a very narrow range of silica contents (Fig. 5), (SiO<sub>2</sub> ranges from 77.8 to 78.9 wt. %). Consistently with a wider range of pumice compositional variations, this range is somewhat wider for melts from the Mendeleev and Golovnin calderas. Groundmass glass compositions of the Golovnin Caldera pumice in Fig. 5 are divided into two groups; one of them is similar in SiO<sub>2</sub> content to melt compositions from Iturup Island and the Mendeleev Caldera eruptions, while the other is much depleted in silica. The latter corresponds to basaltic pumice from a pyroclastic profile on the southeastern outer slope of the caldera.

Comparative analysis of melt inclusions glasses, pumice groundmass, and bulk rock chemistry reveals significant enrichment in SiO<sub>2</sub> and alkalis (Na<sub>2</sub>O + K<sub>2</sub>O), coupled with sharp depletion in CaO, Al<sub>2</sub>O<sub>3</sub>, MgO and FeO in the melt relative to bulk rock data (Fig. 7).

The parental melts for silicic pumice phenocrysts correspond compositionally to low- medium-K calcareous rhyolites (plagiogranites) (Fig. 7). Among these, the Mendeleev and Golovnin calderas melts demonstrate the most K<sub>2</sub>O-depleted signatures. Iturup Island melts contain systematically higher K<sub>2</sub>O contents than their Kunashir counterparts. Among calderas of Iturup Island, the Vetrovoy Isthmus melts are the most K<sub>2</sub>O depleted, while Lvinaya Past and Medvezhiya caldera melts demonstrate K<sub>2</sub>O enrichment.

The findings of combined inclusions in magnesian pyroxenes, represented by rhyolitic glass and amphibole relics, along with significant compositional differences between bulk-rock and melt inclusion glasses, as well as low variability in FeO, MgO, and (in some cases) CaO contents, led to an important conclusion. The formation of melt prior to eruptions in the Vetrovoy Isthmus (Iturup Island) and the Mendeleev Caldera (Kunashir Island) is

likely associated with the peritectic reaction of amphibole decomposition. This process resulted in the formation of peraluminous aluminous plagioryholytic melt, a ‘gabbro-noritic’ restite (composed of high-calcium plagioclase, clinopyroxene, orthopyroxene, and magnetite), and subsequent crystallization of the Ca-rich plagioclase [Smirnov et al., 2019; Kotov et al., 2023].

The peritectic breakdown of amphibole is characteristic of crustal melting during felsic magma formation. The dacitic composition of caldera-forming magmas (e.g., Vetrovoy Isthmus, Mendelev Volcano Caldera, and other late Pleistocene volcanoes) likely results from melt mixing with restite minerals.

Estimates of partial melting conditions indicate that these felsic magmas were generated in the upper island-arc crust (depths <12 km) at temperatures of 810–930 °C [Kotov et al., 2023].

Quartz and plagioclase crystallization temperatures are estimated in the ranges that are similar to the estimates

of partial melting at 830–890 °C and <2–3 kbar [Smirnov et al., 2019; Kotov et al., 2023], i.e. within the depths where the partial melting likely took place.

One of the most important factors contributing to the development of powerful caldera-forming eruptions is the fluid regime of the magmas involved in these processes. The term ‘fluid regime’ refers to the conditions allowing volatile components and fluid phases to exist and interact within magmas. This includes pressure-temperature (P-T) conditions, volatile speciation in the magma, and physical states of fluid phases. The most detailed data shedding light on the fluid regime of GKA caldera-forming eruption magmas are reported in papers on eruptions in the Vetrovoy Isthmus and in the Mendelev Caldera [Smirnov et al., 2019; Kotov et al., 2023]. The melts were volatile-rich, dominated by H<sub>2</sub>O (up to 7.2 wt.%) and Cl (up to 0.4 wt.%), while CO<sub>2</sub> and S occurred only in trace amounts (less than 17 ppm and less than 179 ppm, respectively according to [Kotov et al., 2023]).

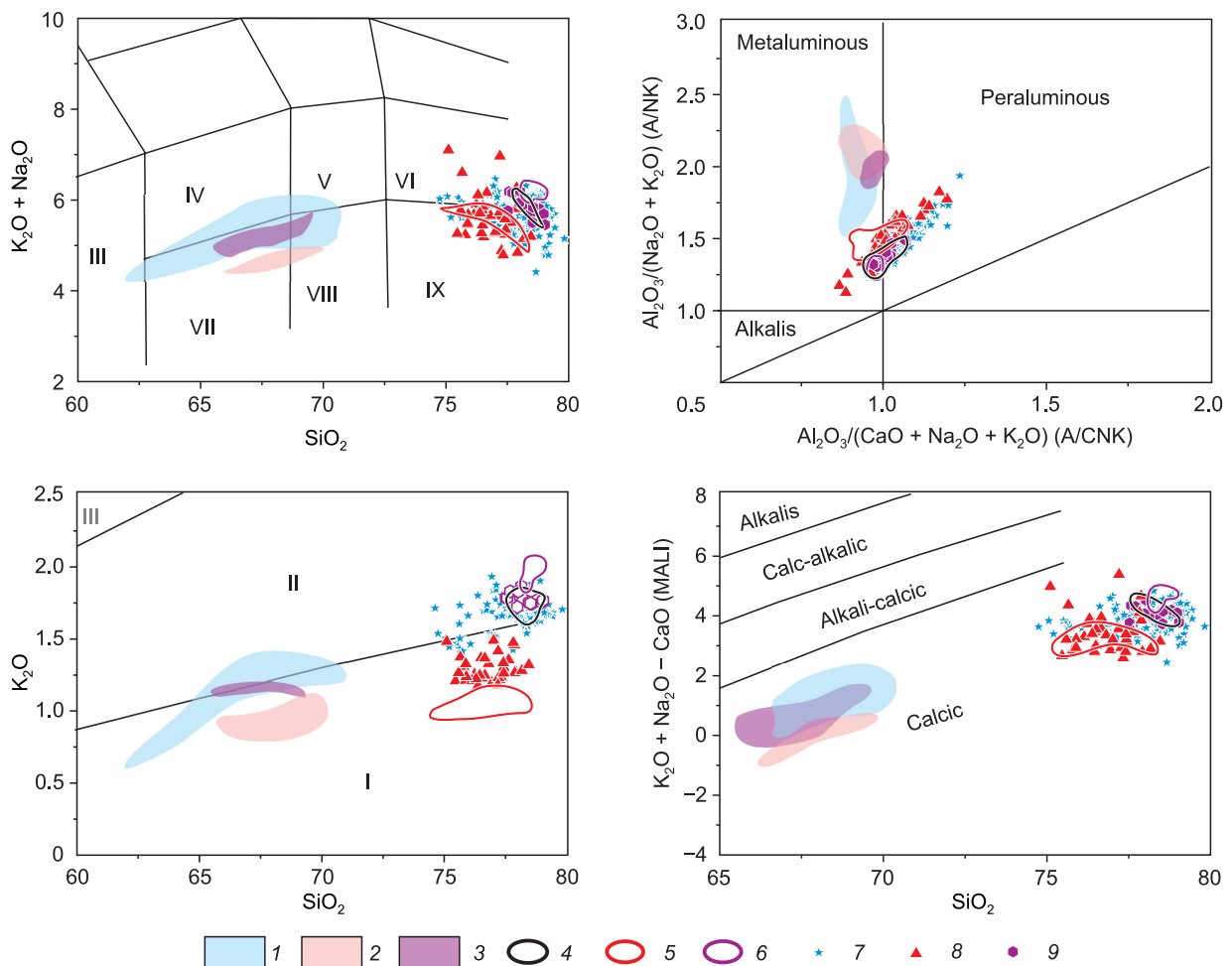


**Fig. 7.** Glass compositions of melt inclusions in pumice minerals from caldera eruptions (GKA Southern Segment), compared to bulk-rock pumice compositions and groundmass glass (wt.%). 1–3 – bulk rock pumice compositions (1 – the Vetrovoy Isthmus (Iturup Island), 2 – the Mendelev Caldera (Kunashir Island), 3 – the Lvinaya Past Caldera (Iturup Island)); 4–6 – groundmass glass compositions from pumice (4 – the Vetrovoy Isthmus, 5 – the Mendelev Caldera, 6 – the Lvinaya Past Caldera); 7–9 – melt inclusion glass compositions (7 – the Vetrovoy Isthmus [Smirnov et al., 2019], 8 – the Mendelev Caldera [Kotov et al., 2023], 9 – the Lvinaya Past Caldera [Smirnov et al., 2017; Kotov et al., 2021]). The symbols are the same as in Fig. 5.

The presence of gas-rich fluid inclusions in plagioclase phenocrysts, less often in pyroxenes, indicates the saturation of melts with fluid. These inclusions were co-trapped with melt inclusions and contain at room temperature a diluted aqueous solution and low-density CO<sub>2</sub>

gas, sometimes with small amounts of H<sub>2</sub>S. Detailed studies of these inclusions [Smirnov et al., 2019] yield a degassing pressure of ~0.9 kbar, corresponding to ~3 km depth in the eruption source.

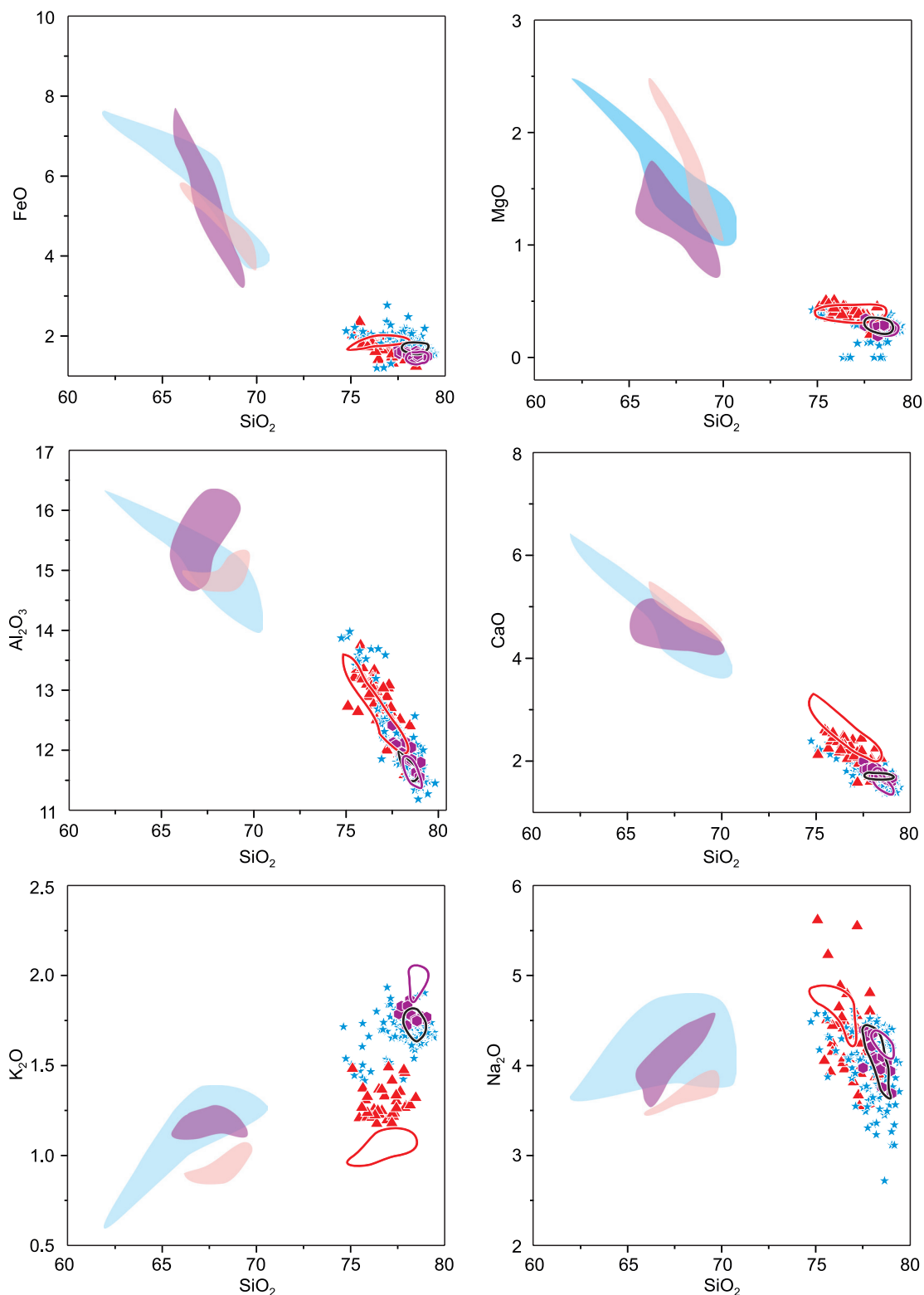


**Fig. 8.** Compositional variations of melt inclusion glass in pumice minerals of caldera eruptions from Southern GKA segment (wt. %). The symbols are the same as in Fig. 7.

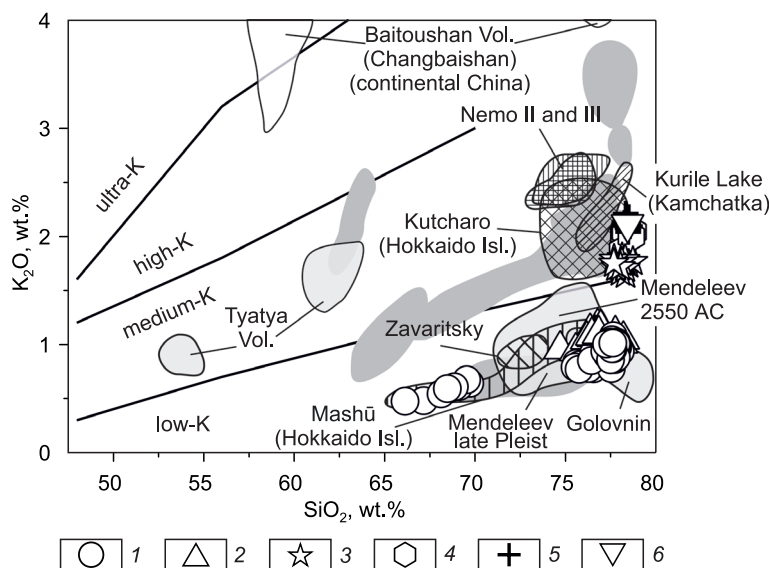


**Fig. 9.** Comparison of glass compositions in pumice and ignimbrite groundmass of GKA caldera volcanoes with those from Hokkaido (Japan) and ash particles in Sea of Okhotsk sediments. The contours of composition fields of proximal tephra volcanic glass from Hokkaido Island (dark gray), South Kuriles (light gray) and Baitoushan/Changbaishan volcano (white), after [Razzhigayeva et al., 2016]; contours of compositional fields of tephra glass from the Sea of Okhotsk sediments (hatching) after [Derkachev et al., 2016]. Proximal pumice and ignimbrite groundmass glass compositions: 1–2 – Kunashir Island (1 – the Golovnin Caldera (authors' data); 2 – the Mendeleev Caldera (authors' data)); 3–5 – Iturup Island (3 – the Vetrovoy Isthmus [Bergal-Kuvikas et al., 2023; Smirnov et al., 2019], 4 – the Lvinaya Past Caldera [Bergal-Kuvikas et al., 2023], 5 – rhyolite pumice of Menshyi Brat Volcano, the Medvezhiya Caldera [Bergal-Kuvikas et al., 2023]; 6 – Onekotan Island, (6 – the Nemo-III Caldera [Melekestsev et al., 1997]).

The data indicate that both magma generation and reservoir emplacement occurred within the upper island-arc crust, with the storage zone situated immediately above and in close proximity to the generation domain. These shallow magma reservoirs hosted  $H_2O-CO_2$ -saturated melts coexisting with a free fluid phase.

#### THE LATE PLEISTOCENE-HOLOCENE CALDERA VOLCANISM OF GKA AND ITS COMPARISON WITH CALDERA FORMATION IN OTHER REGIONS OF THE WORLD

##### Geologic conditions of explosive caldera formation.

The most powerful explosive caldera-forming eruptions of the recent geologic past are predominantly associated with active continental margins (ACM) [Bachmann et al., 2002 (Fish Canyon); Anderson et al., 2000 (Bishop Tuff); De Silva, 1989 (Altiplano-Puna)]. To a lesser extent, they are also typical for volcanic island arcs. The most powerful events occurred within the arcs with mature continental crust (ensialic arcs) [Hughes and Mahood, 2008]. We define 'mature' continental crust as earth's crust comprising sedimentary rocks, metapelitic and metabasitic regionally metamorphosed rocks and intermediate to felsic intrusive bodies [Vitte, 1981]. Examples of explosive calderas in ensialic volcanic arcs are the Toba Caldera in Sumatra [Chesner, 2012] about 74 Ka the Aira Caldera in Kyushu Island 22 Ka. [Aramaki, 1984] and calderas in the Taupō volcanic zone in New Zealand

26.5 Ka [Wilson et al., 1984]. Comparably colossal events in Russia took place in the Pleistocene – Holocene in the Eastern and Southern Kamchatka volcanic zones [Leonov and Grib, 2004; Leonov and Rogozin, 2007; Volyants et al., 1999; Ponomareva et al., 2004].

Volcanic arcs developing on oceanic crust (ensimatic arcs) typically lack the substrates required to generate large volumes of felsic magmas. Nevertheless, calderas 5–10 km in diameter occur in both subaerial and submarine settings across numerous ensimatic arcs [Leat and Larter, 2003; Stern, 2010]. For example, nine Quaternary calderas were identified along the Izu-Ogasawara ensimatic Arc [Lizasa et al., 1999]. Numerous calderas form in other similar island arcs. An example is the submarine Hunga Tonga-Hunga Ha'apai Caldera (Tonga Arc), which hosted the 21st century most powerful explosive but non-caldera forming eruption (VEI ~ 6) [Poli and Shapiro, 2022]. This demonstrates that caldera volcanism may commonly develop in arcs without continental crust.

Explosive caldera volcanism in the Pleistocene – Holocene was typical for the entire GKA. Reliable correlations between caldera distribution and crustal structure remain limited by sparse data on the region's deep structure and intrusive magmatism. Although crustal thickness estimates [Proshkina et al., 2017] and exposed felsic intrusions indicate continental crust both in Northern and Southern segments, the distribution of Quaternary explosion calderas shows striking asymmetry: abundant in the Southern segment, but sparse in the Northern.

Nevertheless, a significant number of explosion calderas are concentrated in the Central GKA segment, where continental crust is presumably absent. Therefore, any direct correlation of explosive caldera formation and the arc crust type remains questionable. Current models suggest that ensimatic volcanic arc crust evolves compositionally from initially oceanic-type characteristics toward continental-type properties during arc maturation - essentially forming distinct island-arc crust [Stern, 2010]. The development of felsic explosive volcanism in the GKA provides a key evidence that it is a mature island-arc. The composition and structure of its crust exhibit transitional characteristics between the oceanic and continental endmembers [Plekhov, 2010].

Notably, the centers of caldera eruptions coincide with the areas of the earth's crust thickening along the eastern margin of the Kuril back-arc basin. This could imply the connection of the late Pleistocene caldera formation with the development of the back-arc basin. Its activity ceased approximately 16–17 Ma [Baranov et al., 2002]. Nevertheless, the spatial distribution of volcanism compared with slab parameters across different GKA segments, along with the magma geochemistry, suggests that these processes continued to affect volcanism and caldera formation in the Southern GKA and Hokkaido Island, even during the Quaternary [Martynov et al., 2015; Bergal-Kuvikas et al., 2024].

The development of dacitic explosive caldera volcanism at the end of the late Pleistocene and Holocene in the Central GKA sector requires further detailed study, taking into account that this part of the arc is anomalous. The Earth's crust in this region is thinner, with rift-like structures transverse to the arc strike observed in the Bussol Strait graben. Seismic structure of the earth crust in the Central segment along with sporadic high-magnitude earthquakes despite its overall lower seismic activity compared to the Northern and Southern sectors may potentially be linked to mantle diapir dynamics [Zlobin et al., 2008; Bergal-Kuvikas et al., 2024]. Thus, in the Central GKA segment, extensional conditions favorable for explosive caldera-forming volcanism could develop, as demonstrated by Leonov and Grib [2004] for the East Kamchatka Volcanic Belt.

While available geochronological data indicate that most Quaternary explosive calderas across GKA formed in the late Pleistocene (<50 Ka), the sparse dating coverage prevents us from confirming this interval as the definitive peak of explosive caldera-forming activity. The older age obtained for the Medvezhiya Caldera indicates that these events may date back to the mid-late Pleistocene, consistent with geomorphology of caldera volcanoes. Nevertheless, it is highly probable that the period of active caldera formation in the GKA was contemporaneous with the peak caldera-forming activity in the East Kamchatka Volcanic Belt and Southern Kamchatka. It is noteworthy that Holocene explosive caldera formation both in Kamchatka and GKA, e.g. Tao-Rusyr Caldera in

Onkotan Island [Melekestsev et al., 1998] and, the last calderas of the Zavaritsky Complex in Simushir Island occurred nearly simultaneous, with ages clustering at 8–6 Ka.

The persistence of late Holocene to recent volcanic activity within some GKA calderas indicates that their magmatic systems remain active today. This necessitates enhanced monitoring employing integrated geophysical, geochemical, and satellite-based approaches.

**Composition of magmas, conditions of their generation and storage.** Our analysis of magma storage conditions of the southern GKA caldera-forming eruptions shows close similarities to well-documented systems including Toba (74 Ka), Santorini (3.6 Ka), Katmai (1912 AD), and Pinatubo (1991 AD). These systems share upper-crustal storage depths (3–10 km) and temperatures (750–1,000 °C) [Hammer et al., 2002; Borisova et al., 2005; Chesner and Luhr, 2010; Cadoux et al., 2014; Geshi et al., 2020]. Petrologic evidence confirms that some caldera-forming eruptions were triggered by hotter mafic or andesitic recharge of felsic magma reservoirs [Sparks et al., 1977; Simon et al., 2014].

Modern local seismic tomography of Pleistocene-Holocene calderas at convergent margins typically reveals small shallow magma reservoirs at depths of 2–15 km [Huang et al., 2015, 2018; Kasatkina et al., 2022; Koulikov et al., 2023; Giacomuzzi et al., 2024]. Most of them represent either remnant chambers from caldera-forming events, or newly formed reservoirs beneath post-caldera stratovolcanoes. Notable exceptions include large, potentially active systems like Yellowstone and Campi Flegrei, where seismic tomography detects voluminous melt accumulations capable of future caldera-scale eruptions [Huang et al., 2015; Giacomuzzi et al., 2024].

Felsic magmas generating caldera-forming eruptions are typically enriched in water, with melts containing from 2 to 8 wt.% of H<sub>2</sub>O, which, along with the above-mentioned estimates of the storage depth and pressures, suggest a nearly aqueous fluid saturated state. Elevated water contents and presence of a fluid phase in the caldera-forming eruption magmas were repeatedly confirmed by fluid and melt inclusion studies [Plekhov et al., 2010; Borisova et al., 2014; Smirnov et al., 2019]. Shallow (~3km) magma degassing may become an independent caldera eruption trigger. The released fluid expands dramatically, generating overpressure at the reservoir roof. This results in a roof rupture and initiates runaway decompression degassing, violent magma fragmentation and the catastrophic expulsion of a fluidized mixture of magmatic melt, crystals and shattered host rocks through multiple vents and ring faults. Data on fluid regime of GKA caldera-forming eruptions could form the basis for a predictive scientific framework for this type of events. Our research demonstrates that even eruptions with comparable magma reservoirs (Lvinaya Past Caldera and Vetrovoy Isthmus, Iturup Island) can diverge radically in water dynam-

ics, challenging assumptions about uniform pre-eruptive volatile behavior [Smirnov et al., 2017, 2019].

Caldera formation at convergent plate boundaries is nearly universally linked to eruptions of felsic magmas – specifically of dacitic, rhyodacitic and rhyolitic compositions [Bergal-Kuvikas et al., 2019]. Moreover, the volumes of eruptions suggest batholith sized reservoir volumes [Annen, 2009].

Fractionation of more primitive, frequently mafic magmas, variably modified by crustal assimilation [Gill, 1981; Gertisser and Keller, 2005; Volynets et al., 1999], and partial melting of crustal rocks [Laube and Springer, 1998; Beard and Lofgren, 1991; Atherton and Petford, 1993; Haraguchi et al., 2017] are regarded as the dominant mechanisms generating felsic magmas. Fractionation of mafic and intermediate magmas seems to be predominant, since volcanoes at convergent plate boundaries erupt generally andesitic and basaltic lavas and pyroclastics. Nevertheless, generating evolved silicic melts in arc settings would demand an implausibly high degree (70–85%) of fractional crystallization from primitive parent magma [Kawamoto, 1996; Nandedkar et al., 2014]. Large volumes of felsic caldera-forming eruptions, thus, challenge in many cases geological viability of fractional crystallization, even if it involves a crustal rock assimilation, as a sole petrogenetic mechanism.

In ACM settings, the presence of metapelites and pre-existing felsic-intermediate intrusive rocks provides unquestionable potential for generating significant volumes of felsic melt through a crustal anatexis. However, in the island arcs like GKA, producing voluminous silicic melts appears geochemically difficult due to the dominantly mafic, i.e. lower  $\text{SiO}_2$ ,  $\text{Al}_2\text{O}_3$ ,  $\text{Na}_2\text{O}$  and  $\text{K}_2\text{O}$  contents, compositions of the crustal rocks.

Mineralogical and fluid/melt inclusion studies of pumice from powerful caldera-forming eruptions on Iturup and Kunashir islands indicate that magma-generation involved dehydration melting of amphibole-bearing metabasic rocks in the upper part of arc crust, producing plagioryholitic melts and ‘gabbro-noritic’ restite. The evolution of this magma involved subsequent crystallization of new plagioclase from melt and late-stage quartz crystallization. The consistency of these processes across diverse island-arc caldera systems implies that they may constitute a universal mechanism for both generation and subsequent evolution of large-volume silicic magmas in island arc environments [Kotov et al., 2023].

However, assuming low felsic melt productivity (10–20%) of metabasic rock anatexis [Beard and Lofgren, 1992; Gao et al., 2016], forming large magma reservoirs requires long-lived thermal influence on the crustal rocks to permit incremental accumulation of melts or existence of massive melting domains to compensate low yield. Thermomechanical modeling demonstrates that repeating injections of intermediate-composition dikes into the arc crust can facilitate either incremental partial melt accumulation over multiple intrusion events [Annen and

Sparks, 2002], or thermal priming of lower crustal rocks, enabling partial melting [Petford and Gallagher, 2001]. This should generate sufficiently large felsic melt volumes at geologically viable timescales. The timescales required for the formation of magma reservoirs beneath GKA caldera volcanoes remain poorly constrained by current data. Thermomechanical modeling suggests that the development of a crustal magma reservoir capable of fueling large explosive eruption requires  $10^5$ – $10^6$  years [Petford and Gallagher, 2001; Karakas and Dufek, 2015]. However, total active lifespans of magma reservoirs feeding the caldera-forming eruption in the GKA remain largely unknown. Recent findings from the Vertovoy Isthmus reveal that the magma system, which was likely responsible for formation of late Pleistocene pumice deposits, remained active as recently as ~2,000 years BP, producing another powerful eruption (VEI about 4–5) [Bergal-Kuvikas et al., 2023]. This necessitates assessment of possible consequences of such eruptions and volcanic hazards associated with caldera volcanoes in the Southern GKA sector. Furthermore, recent seismic tomography data reveals high  $V_p/V_s$  anomaly in the central part of Iturup Island at a depth ~5 km. This anomaly may represent remnants of magma and/or fluid accumulations that likely fed both explosive eruptions in the Vetrovoy Isthmus area [Koulakov et al., 2024].

## CONCLUSIONS

The review demonstrated that caldera-forming eruptions occurred throughout all GKA segments in the late Pleistocene and Holocene. They were most frequent in the Southern and Central segments – particularly where the volcanic arc meets the back-arc Kuril Basin. Explosive caldera volcanism was significantly weaker in the Northern segment and entirely absent on Paramushir Island (the region’s second largest island). The reasons of this spatial variability remains unclear and require further detailed study.

The currently available geochronological data are insufficient to build a comprehensive timeline of GKA caldera-forming eruptions during the Quaternary period. However, they suggest that it could be divided into two possible stages, similar to Quaternary calderas in East and South Kamchatka volcanic belts: the most intense at the late Pleistocene (50–12 Ka), and the less intense in the early Holocene (8–6 Ka). The possible powerful caldera-forming eruptions at earlier dates and prolonged Holocene activity may have occurred but remain unconfirmed. To clarify the GKA caldera volcanism chronology, expanded paleovolcanologic and geochronologic research, including a detailed analysis of the proximal pyroclastic deposits and correlation of distal tephra layers in terrestrial and marine records around GKA islands, are necessary.

Caldera-forming eruptions, even smaller ones, represent high-impact events with multi-scale environmental

consequences. Proximal pyroclastic density currents and massive ashfalls can completely obliterate existing ecosystems, sometimes including the flora and fauna extinctions. Distal impacts involve stratospheric volcanic ash and aerosol loading, which may cause a global radiative forcing ultimately decreasing average annual temperatures (the effect of the ‘volcanic winter’). Systematic study of the GKA caldera eruption impacts on ecosystems could significantly refine modern volcanic risk models.

Recent advances in petrological research suggest that the formation of GKA calderas in the late Pleistocene and Holocene was linked to large felsic magma reservoirs developed in the upper island-arc crust (3–12 km). The dominant dacitic compositions exhibit clear petrogenetic affinities to M-type granitoids [White, 1979], which form primarily through partial melting of metabasitic upper crustal rocks at temperatures below 950 °C. The mechanisms and spatial-temporal scales of felsic magma generation in the upper GKA island-arc crust remain poorly constrained and require further systematic study. This process may be driven by prolonged (~1 Myr) repetitive intrusions of high-temperature basic to intermediate magmas into the arc crust. Detailed analysis of post-caldera volcanic products could provide critical insights into crustal melting triggers and melt extraction processes.

Existing data remains insufficient to characterize the present-day state of magmatic systems capable of producing catastrophic caldera-forming eruptions due to sparse monitoring data. Establishing seismic monitoring networks and advancing tomographic imaging techniques on caldera volcanoes, creation seismic tomography models of their feeding systems are prerequisite for development effective early warning systems and mitigating risks associated with their potential reactivation.

Rhyolitic melts of dacitic magmas in caldera-forming eruptions were typically saturated with H<sub>2</sub>O, CO<sub>2</sub>, sulfur species and, likely, other volatile components. This volatile enrichment promoted extensive degassing during pre-eruptive magma evolution. Available constraints indicate that these processes predominantly occurred at shallow crustal depths (~3 km). However, some uncertainties persist concerning influence of volatile components on the entire process of preparing of catastrophic eruptions. The early stage degassing in the magma reservoir could serve as an independent trigger for a powerful explosive eruption and caldera collapse. There is also no complete certainty in understanding the sources of volatile components: dehydration partial melting of the crustal rocks or degassing of deep magmas. Resolving these questions requires further detailed research in petrology of GKA felsic magmas and fluid behavior in the magma reservoirs of caldera-forming eruptions.

#### ACKNOWLEDGEMENTS AND FUNDING

Original data on whole rock compositions, compositions of groundmass glass and melt inclusions were ob-

tained at the laboratories of the Center for Multi-elemental and Isotopic Research (IGM SB RAS, Novosibirsk). This work was supported by the Government Contract of V.S. Sobolev Institute of Geology and Mineralogy (IGM SB RAS, Novosibirsk), Institute of Volcanology and Seismology (IVS FEB RAS, Petropavlovsk-Kamchatsky), Institute of Marine Geology and Geophysics (IMGG FEB RAS, Yuzhno-Sakhalinsk). Some materials were collected due to the support of the Kurilsky Natural Reserve (Yuzhno-Kurilsk, Sakhalin oblast).

The authors express their profound gratitude to the reviewers Dr. P.Yu. Plechov (A.E. Fersman Mineralogical Museum, RAS, Moscow) and Dr. A.B. Perepelov (IGM SB RAS, Irkutsk) for their valuable comments and suggestions that substantially improved the manuscript.

This paper is dedicated to Dr. Yu.A. Martynov and Dr. A.V. Rybin, outstanding researchers of Kuril Islands volcanism.

#### REFERENCES

- Afanasev, V.V., Dunaev, N.N., Gorbunov, A.O., Uba, A.V. (2020). The Manifestation of caldera-forming Volcanism in the Formation of the Coast (On Example of Iturup Island of the Great Kuril Ridge), in: Chaplina, T.O. (Ed.). Processes in GeoMedia, Volume I. Springer Geology, Springer, pp. 51–61, DOI: [10.1007/978-3-030-38177-6\\_7](https://doi.org/10.1007/978-3-030-38177-6_7).
- Anderson, A.T., Davis, A.M., Lu, F. (2000). Evolution of Bishop Tuff rhyolitic magma based on melt and magnetite inclusions and zoned phenocrysts. *Journal of Petrology* 41 (3), 449–473, DOI: [10.1093/petrology/41.3.449](https://doi.org/10.1093/petrology/41.3.449).
- Annen, C. (2009). From plutons to magma chambers: thermal constraints on the accumulation of eruptible silicic magma in the upper crust. *Earth and Planetary Science Letters* 284, 409–416, DOI: [10.1016/j.epsl.2009.05.006](https://doi.org/10.1016/j.epsl.2009.05.006).
- Annen, C., Sparks, R.S.J. (2002). Effects of repetitive emplacement of basaltic intrusions on thermal evolution and melt generation in the crust. *Earth and Planetary Science Letters* 203, 937–955, DOI: [10.1016/S0012-821X\(02\)00929-9](https://doi.org/10.1016/S0012-821X(02)00929-9).
- Aramaki, S. (1984). Formation of the Aira Caldera, Southern Kyushu, 22,000 Years Ago. *Journal of Geophysical Research* 89 (B10), 8485–8501, DOI: [10.1029/JB089IB10P08485](https://doi.org/10.1029/JB089IB10P08485).
- Atherton, M.P., Petford, N. (1993). Generation of sodium-rich magmas from newly underplated basaltic crust. *Nature* 362, 144–146, DOI: [10.1038/362144a0](https://doi.org/10.1038/362144a0).
- Avdeiko, G.P., Antonov, A.Y., Volynets, O.N. (1992). Submarine volcanism and zonation of the Kuril Island Arc. Nauka, Moscow, [in Russian].
- Bachmann, O., Bergantz, G. (2008). The magma reservoirs that feed supereruptions. *Elements* 4 (1), 17–21, DOI: [10.2113/GSELEMENTS.4.1.17](https://doi.org/10.2113/GSELEMENTS.4.1.17).
- Bachmann, O., Dungan, M., Lipman, P.W. (2002). San Juan volcanic field, Colorado: rejuvenation and eruption of an upper-crustal batholith. *Journal of Geophysical Research* 43 (8), 1469–1503.
- Baranov, B., Wong, H. K., Dozorova, K., Karp, B., Ludmann, T., Karnaukh V. (2002). Opening geometry of the Kurile Basin (Okhotsk Sea) as inferred from structural data. *Island Arc* 11 (3), 206–219, DOI: [10.1046/j.1440-1738.2002.00366.x](https://doi.org/10.1046/j.1440-1738.2002.00366.x).
- Barker, F. (1979). Trondhjemite: definition, environment and hypotheses of origin, in: Barker, F. (Ed.). *Trondhjemites, dacites and related rocks*. Elsevier, New York, pp. 1–12.
- Bazanov, L.L., Melekestsev, I.V., Ponomareva, V.V., Dirksen, O.V., Dirksen, V.G. (2016). Late Pleistocene and Holocene volcanic catastrophes in Kamchatka and in the Kuril Is-

- lands. Part 1. Types and classes of catastrophic eruptions as the leading components of volcanic catastrophism. *Journal of Volcanology and Seismology* 10 (3), 151–169, DOI: [10.1134/S0742046316030027](https://doi.org/10.1134/S0742046316030027).
- Beard, J.S., Lofgren, G.E. (1991).** Dehydration melting and water-saturated melting of basaltic and andesitic greenstones and amphibolites. *Journal of Petrology* 32, 365–401, DOI: [10.1093/ptrology/32.2.365](https://doi.org/10.1093/ptrology/32.2.365).
- Bergal-Kuvikas, O.V. (2015).** Volume of Quaternary volcanic material of the Kuril Island Arc: analysis of spatial variations in correlation with subduction zone. *Russian Journal of Pacific Geology*, 34 (2), 103–116.
- Bergal-Kuvikas, O.V., Gordeev, E.I. & Koulakov, I.Y. (2024).** The role of the back-arc basin in the formation of slab heterogeneity and the origin of volcanism in the Kuril–Kamchatka Island Arc. *Doklady of the Earth Sciences* 516, 1010–1014, DOI: [10.1134/S1028334X2460141X](https://doi.org/10.1134/S1028334X2460141X).
- Bergal-Kuvikas, O.V., Smirnov, S.Z., Agatova, A.R. (2023).** The Holocene explosive eruption on Vetrovoi Isthmus (Iturup Island) as a source of the marker tephra Layer of 2000 cal. yr BP in the Central Kuril Island Arc. *Doklady Earth Sciences* 511, 550–557, DOI: [10.1134/S1028334X23600597](https://doi.org/10.1134/S1028334X23600597).
- Bergal-Kuvikas, O.V., Rogozin A.N., Klyapitsky E.S. (2019).** The analysis of spatial distributions, origins of caldera-forming eruptions with basaltic-andesitic magma compositions, and genesis of Miocene ignimbrites of the Eastern volcanic belt, Kamchatka. *Geodynamics & Tectonophysics* 10 (3), 815–828, DOI: [10.5800/GT-2019-10-3-0443](https://doi.org/10.5800/GT-2019-10-3-0443).
- Bondarenko, V.I. (1991).** Seismic reflection profiling in Lake Kurilskoe. *Volcanology & Seismology* 12 (4), 533–548.
- Bondarenko, V.I., Rashidov, V.A. (2003).** The Chernye Bratya volcanic massif, Kurile Is. *Volcanology & Seismology* 3, 35–51.
- Bondarenko, V.I., Rashidov, V.A. (2018).** The Structure of the Ushishir Volcanic Massif, Central Kurils. *Journal of Volcanology and Seismology* 12, 16–33, DOI: [10.1134/S0742046318010025](https://doi.org/10.1134/S0742046318010025).
- Borisova, A.Y., Pichavant, M., Beny, J.M., Rouer, O., J.P. (2005).** Constraints on dacite magma degassing and regime of the June 15, 1991, climactic eruption of Mount Pinatubo (Philippines): New data on melt and crystal inclusions in quartz. *Journal of Volcanology and Geothermal Research* 145(1), 35–67, DOI: [10.1016/j.jvolgeores.2005.01.004](https://doi.org/10.1016/j.jvolgeores.2005.01.004).
- Borisova, A.Y., Toutain, J.P., Dubessy, J., Pallister, J., Zwick, A., Salvi, S. (2014).** H<sub>2</sub>O-CO<sub>2</sub>-S fluid triggering the 1991 Mount Pinatubo climactic eruption (Philippines). *Bulletin of Volcanology* 76, 800, DOI: [10.1007/s00445-014-0800-3](https://doi.org/10.1007/s00445-014-0800-3).
- Braitseva, O.A., Melekestsev, I.V., Ponomareva, V., Sulerzhitsky, L.D. (1995).** Ages of calderas, large explosive craters and active volcanoes in the Kuril-Kamchatka region, Russia. *Bulletin of Volcanology* 57, 383–402, DOI: [10.1007/BF00300984](https://doi.org/10.1007/BF00300984).
- Bronk Ramsey, C. (1995).** Radiocarbon calibration and analysis of stratigraphy: the OxCal program. *Radiocarbon* 37 (2), 425–430, DOI: [10.1017/s0033822200030903](https://doi.org/10.1017/s0033822200030903).
- Bulgakov, R.F. (2018).** Application of thermoluminescence dating for pyroclastic deposits on the Kuril Islands. *Geosystems of Transition Zones* 2 (4), 392–397, DOI: [10.30730/2541-8912.2018.2.4.392-397](https://doi.org/10.30730/2541-8912.2018.2.4.392-397).
- Cadoux, A., Scaillet, B., Druitt, T. H., Deloule, E. (2014).** Magma storage conditions of large Plinian eruptions of Santorini volcano (Greece). *Journal of Petrology* 55, 1129–1171, DOI: [10.1093/ptrology/egu021](https://doi.org/10.1093/ptrology/egu021).
- Chesner, C.A. (2012).** The Toba Caldera complex. *Quaternary International* 258, 5–18, DOI: [10.1016/j.quaint.2011.09.025](https://doi.org/10.1016/j.quaint.2011.09.025).
- Chesner, C.A., Luhr, J.F. (2010).** A melt inclusion study of the Toba Tuffs, Sumatra, Indonesia. *Journal of Volcanology and Geothermal Research* 197, 259–278, DOI: [10.1016/j.jvolgeores.2010.06.001](https://doi.org/10.1016/j.jvolgeores.2010.06.001).
- Cole, J.W., Milner, D.M., Spinks, K.D. (2005).** Calderas and caldera structures: a review. *Earth-Science Reviews* 69 (1), 1–26, DOI: [10.1016/j.earscirev.2004.06.004](https://doi.org/10.1016/j.earscirev.2004.06.004).
- De Silva, S. L. (1990).** Altiplano-Puna volcanic complex of the central Andes. *Geology* 17 (12), 1102–1106, DOI: [10.1130/0091-7613\(1989\)017%3C.](https://doi.org/10.1130/0091-7613(1989)017%3C.)
- Degtarev, A.V., Rybin, A.V., Melekestsev, I.V., Razzhigaeva, N.G. (2012).** Explosive eruptions of the Sarychev Peak Volcano in the Holocene on Matua Island, the Central Kuriles: the tephra geochemistry. *Russian Journal of Pacific Geology* 6 (6), 423–432, DOI: [10.1134/S1819714012060024](https://doi.org/10.1134/S1819714012060024).
- Degtarev, A.V., Rybin, A.V., Arslanov, K.A., Koroteev, I.G., Guryanov, V.B., Kozlov, D.N., Chibisova, M.V. (2015).** Catastrophic explosive eruptions of Lvinaya Past' (Iturup Island): stratigraphy and geochronology, in: Levin, B.V., Likhacheva, O.N. (Eds.). *Geodynamic Processes and Natural Hazards. Neftegorsk Experience*. Dalnauka, Vladivostok, pp. 210–213.
- Derkachev, A.N., Portnyagin, M.V. (2013).** Marker tephra layers in the late Quaternary deposits of the Sea of Okhotsk as evidence of catastrophic eruptions in the Nemo caldera complex (Onekotan Island, Kuril Islands). *Stratigraphy and Geological Correlation* 21 (5), 553–571, DOI: [10.1134/S0869593813040035](https://doi.org/10.1134/S0869593813040035).
- Derkachev, A.N., Nikolaeva, N.A., Gorbarenko, S.A., Portnyagin, M.V., Ponomareva, V.V., Nürnberg, D., Sakamoto, T., Iijima, K., Liu, Y., Shi, X., Lv, H., Wang, K. (2016).** Tephra layers in the quaternary deposits of the Sea of Okhotsk: Distribution, composition, age and volcanic sources. *Quaternary International* 425, 248–272, DOI: [10.1016/J.QUAINT.2016.07.004](https://doi.org/10.1016/J.QUAINT.2016.07.004).
- Dirksen, O.V., Rybin, A.V. (2018).** Explosive eruptions of Zavaritsky Caldera as a possible source of ashes in marine cores of the NW Pacific, in: *Volcanism and Related Processes. Materials of the XXI Regional Scientific Conference dedicated to Volcanologist's Day*. Institute of Volcanology and Seismology, FEB RAS, Petropavlovsk-Kamchatsky, pp. 40–43, [in Russian].
- Dirksen, O.V., Rybin, A.V. (2020).** Early Holocene tephra of Zavaritsky Caldera (Simushir Island): new ash markers of the NW Pacific, in: *Volcanism and Related Processes. Materials of the XXIII Annual Scientific Conference dedicated to Volcanologist's Day*. Institute of Volcanology and Seismology, FEB RAS, Petropavlovsk-Kamchatsky, pp. 18–21, [in Russian].
- Erlich, E. (1986).** Geology of the calderas of Kamchatka and Kurile Islands with comparison to calderas of Japan and the Aleutians, Alaska. U.S. Geological Survey, Open-File Report 86–291, DOI: [10.3133/ofr86291](https://doi.org/10.3133/ofr86291).
- Erlich, E.N., Melekestsev, I.V. (1973).** Quaternary volcanism of the western part of the Pacific Ring of Fire, in: Rudich, K.N. (Ed.). *Acidic volcanism*. Nauka, Novosibirsk, pp. 4–39, [in Russian].
- Ermakov, V.A., Semakin, V.P. (1996).** Geology of Medvezhya Caldera (Iturup Island, Kuril Islands). *Doklady Earth Sciences* 351 (3), 361–365.
- Ermakov, V.A., Steinberg, G.S. (1999).** Kudryavyy volcano and evolution of Medvezhya caldera (Iturup I., Kuril IIs.) *Volcanology and Seismology* 3, 19–40.
- Fedorchenko, V.I., Abdurakhmanov, A.I., Rodionova, R.I. (1989).** Volcanism of the Kuril Island Arc: geology and petrogenesis. Nauka, Moscow, [in Russian].
- Frost, B.R., Barnes, C.G., Collins, W.J., Arculus, R.J., Ellis, D.J., Frost, C.D. (2001).** A geochemical classification for granitic rocks. *Journal of Petrology* 42 (11), 2033–2048, DOI: [10.1093/ptrology/42.11.2033](https://doi.org/10.1093/ptrology/42.11.2033).
- Gao, P., Zheng, Y.F., Zhao, Z.F. (2016).** Experimental melts from crustal rocks: A lithochemical constraint on granite petrogenesis. *Lithos* 266–267, 133–157, DOI: [10.1016/j.lithos.2016.10.005](https://doi.org/10.1016/j.lithos.2016.10.005).
- Gertisser, R., Keller, J. (2000).** From basalt to dacite: origin and evolution of the calc-alkaline series of Salina, Aeolian Arc, Italy. *Contributions to Mineralogy and Petrology* 139 (5), 607–626, DOI: [10.1007/s004100000159](https://doi.org/10.1007/s004100000159).
- Geshi, N., Yamada, I., Matsumoto, K., Nishihara, A., Miyagi, I. (2020).** Accumulation of rhyolite magma and triggers for a caldera-forming eruption of the Aira Caldera, Japan. *Bulletin of Volcanology* 82 (6), DOI: [10.1007/s00445-020-01384-6](https://doi.org/10.1007/s00445-020-01384-6).

- Giacomuzzi, G., Chiarabba, C., Bianco, F., De Gori, P., Agostinetti, N.P. (2024).** Tracking transient changes in the plumbing system at Campi Flegrei Caldera. *Earth Planetary Science Letters* 637, 118744, DOI: [10.1016/j.epsl.2024.118744](https://doi.org/10.1016/j.epsl.2024.118744).
- Gill, J.B. (1981).** *Orogenic Andesites and Plate Tectonics*. Springer-Verlag, Berlin.
- Giordano, G., Cas, R.A.F. (2021).** Classification of ignimbrites and their eruptions. *Earth-Science Reviews* 220, 103697, DOI: [10.1016/j.earscirev.2021.103697](https://doi.org/10.1016/j.earscirev.2021.103697).
- Gorshkov, G.S. (1958).** Active volcanoes of the Kuril Island Arc, in: *Young volcanism of the USSR* [in Russian]. Proceedings of the Laboratory of Volcanology of the USSR Academy of Sciences. Publishing House of USSR Academy of Sciences 13, Moscow, pp. 5–70.
- Gorshkov, G.S. (1960).** Zavaritsky Caldera [in Russian]. *Bulletin of Volcanic Station* 30, 30–49.
- Gorshkov, G.S. (1961).** Fused tuff of Zavaritsky Caldera (Simushir Island, Kuril Islands) [in Russian], in: *Proceedings of the Laboratory of Volcanology of the USSR Academy of Sciences*, 20, pp. 102–107.
- Gorshkov, G.S. (1967).** *Volcanism of the Kuril Island Arc*. Nauka, Moscow, [in Russian].
- Hammer, J.E., Rutherford, M.J., Hildreth, W. (2002).** Magma storage prior to the 1912 eruption at Novarupta, Alaska. *Contributions to Mineralogy and Petrology* 144 (2), 144–162, DOI: [10.1007/s00410-002-0393-2](https://doi.org/10.1007/s00410-002-0393-2).
- Haraguchi, S., Kimura, J.I., Senda, R., Fujinaga, K., Nakamura, K., Takaya, Y., Ishii, T. (2017).** Origin of felsic volcanism in the Izu arc intra-arc rift. *Contributions to Mineralogy and Petrology* 172 (5), 25, DOI: [10.1007/s00410-017-1345-1](https://doi.org/10.1007/s00410-017-1345-1).
- Huang, H.H., Lin, F.C., Schmandt, B., Farrell, J., Smith, R. B., Tsai, V.C. (2015).** The Yellowstone magmatic system from the mantle plume to the upper crust. *Science* 348 (6236), 773–776, DOI: [10.1126/science.aaa5648](https://doi.org/10.1126/science.aaa5648).
- Huang, Y.C., Ohkura, T., Kagiya, T., Yoshikawa, S., Inoue, H. (2018).** Shallow volcanic reservoirs and pathways beneath Aso caldera revealed using ambient seismic noise tomography. *Earth, Planets and Space* 70 (1), 169, DOI: [10.1186/s40623-018-0941-2](https://doi.org/10.1186/s40623-018-0941-2).
- Hughes, G.R., Mahood, G.A. (2008).** Tectonic controls on the nature of large silicic calderas in volcanic arcs. *Geology* 36 (8), 627–630, DOI: [10.1130/G24796A.1](https://doi.org/10.1130/G24796A.1).
- Iizasa, K., Fiske, R.S., Ishizuka, O., Yuasa, M., Hashimoto, J., Ishibashi, J., Naka, J., Horii, Y., Fujiwara, Y., Imai, A., Koyama, S. (1999).** A Kuroko-type polymetallic sulfide deposit in a submarine silicic caldera. *Science* 283 (5404), 975–977, DOI: [10.1126/science.283.5404.975](https://doi.org/10.1126/science.283.5404.975).
- Karakas, O., Dufek, J. (2015).** Melt evolution and residence in extending crust: Thermal modeling of the crust and crustal magmas. *Earth Planetary Science Letters* 425, 131–144, DOI: [10.1016/j.epsl.2015.06.001](https://doi.org/10.1016/j.epsl.2015.06.001).
- Kasatkina, E., Koulakov, I., Grapenthin, R., Izbekov, P., Larsen, J.F., Al Arifi, N., Qaysi, S.I. (2022).** Multiple magma sources beneath the Okmok caldera as inferred from local earthquake tomography. *Journal of Geophysical Research, Solid Earth* 127 (10), DOI: [10.1029/2022JB024656](https://doi.org/10.1029/2022JB024656).
- Kawamoto, T. (1996).** Experimental constraints on differentiation and H<sub>2</sub>O abundance of calc-alkaline magmas. *Earth Planetary Science Letters* 144 (3–4), 577–589.
- Korsunskaya, G.V. (1956).** Volcanoes of Simushir Island [in Russian]. *Bulletin of Volcanic Station* 24, 61–65.
- Kotov, A.A., Smirnov, S.Z., Plechov, P.Y., Persikov, E.S., Chertkova, N.V., Maksimovich, I.A., Karmanov, N.S., Buhtiyarov, P.G. (2021).** Method for determining water content in natural rhyolitic melts by Raman spectroscopy and electron microprobe analysis. *Petrology* 29 (4), 386–403, DOI: [10.1134/S0869591121040044](https://doi.org/10.1134/S0869591121040044).
- Kotov, A., Smirnov, S., Nizametdinov, I., Uno, M., Tsuchiya, N., Maksimovich, I. (2023).** Partial melting under shallow-crustal conditions: a study of the Pleistocene caldera eruption of Mendeleev Volcano, Southern Kuril Island Arc. *Journal of Petrology* 64 (6), DOI: [10.1093/ptrology/egad033](https://doi.org/10.1093/ptrology/egad033).
- Koulakov, I., Izbekov, P., Eichelberger, J., Al Arifi, N., Qaysi, S. I. (2023).** Interconnection of magma sources beneath the Katmai volcanic system inferred from seismic tomography and petrology. *Journal of Volcanology and Geothermal Research* 434, 107744, DOI: [10.1016/j.jvolgeores.2023.107744](https://doi.org/10.1016/j.jvolgeores.2023.107744).
- Koulakov, I., Gordeev, E.I., Abkadyrov, I., Bergal-Kuvikas, O., Chebrov, D. (2024).** Feeding system beneath active volcanoes in central part of Iturup Island (Kuril Arc) inferred from local earthquake tomography. *Journal of Volcanology and Geothermal Research* 456, 108233, DOI: [10.1016/j.jvolgeores.2024.108233](https://doi.org/10.1016/j.jvolgeores.2024.108233).
- Kovtunovich, P.Y., Safronov, A.D., Udodov, V.V., Kudelkin, V.V. (2002).** State Geological Map of Russian Federation. Scale 1: 200,000. Kuril Series. VSEGEI, St. Petersburg.
- Kuzmin, D.V., Nizametdinov, I.R., Smirnov, S.Z., Timina, T.Y., Shevko, A.Y., Gora, M.P., Rybin, A.V. (2023).** Magnesian basalts of the Medvezhia Caldera: main magmas and their sources on the example of the Menshiy Brat Volcano (Iturup Island), Kuriles. *Petrology* 31 (3), 238–263, DOI: [10.1134/S0869591123030062](https://doi.org/10.1134/S0869591123030062).
- Laube, N., Springer, J. (1998).** Crustal melting by ponding of mafic magmas: A numerical model. *Journal of Volcanology and Geothermal Research* 81 (1–2), 19–35, DOI: [10.1016/S0377-0273%2897%2900072-3](https://doi.org/10.1016/S0377-0273%2897%2900072-3).
- Laverov, N. P. (Ed.) (2005).** *Modern and Holocene Volcanism in Russia* [in Russian]. Nauka, Moscow.
- Leat, P.T., Larter, R.D. (2003).** Intra-oceanic subduction systems: introduction. *Geological Society, London Special Publications*, 219 (1), 1–17, DOI: [10.1144/GSL.SP.2003.219.01.01](https://doi.org/10.1144/GSL.SP.2003.219.01.01).
- Leonov, V.L., Grib, E.N. (2004).** Structural Positions and Volcanism of the Quaternary Calderas of Kamchatka. *Dal'nauka, Vladivostok*.
- Leonov, V.L., Rogozin, A.N. (2007).** Karymshina, A giant supervolcano caldera in Kamchatka: boundaries, structure, volume of pyroclastics. *Journal of Volcanology and Seismology* 1 (5), 14–28, DOI: [10.1134/S0742046307050028](https://doi.org/10.1134/S0742046307050028).
- Luchitsky, I.V. (1971).** *Fundamentals of Paleovolcanology. Modern Volcanoes. Vol.1* [in Russian]. Nauka, Moscow.
- Markhinin, E.K. (1959).** Volcanoes of Kunashir Island, in: *Proceedings of the Laboratory of Volcanology of the USSR Academy of Sciences*, Publishing House of the USSR Academy of Sciences 17, 64–155.
- Martynov, A.Y., Martynov, Y.A. (2017).** Pleistocene basaltic volcanism of Kunashir Island (Kuril Island arc): mineralogy, geochemistry, and results of computer simulation. *Petrology* 25 (2), 206–225, DOI: [10.1134/S0869591117020035](https://doi.org/10.1134/S0869591117020035).
- Martynov, A.Y., Martynov, Y.A., Rybin, A.V., Kimura, J.-I. (2015).** Role of back-arc tectonics in the origin of subduction magmas: new Sr, Nd, and Pb isotope data from middle Miocene lavas of Kunashir Island (Kurile Island Arc). *Russian Geology and Geophysics* 56 (3), 363–378, DOI: [10.1016/j.rgg.2015.02.001](https://doi.org/10.1016/j.rgg.2015.02.001).
- Martynov, Y., Rybin, A., Chibisova, M., Ostapenko, D., Davydova, M. (2023).** Basaltic volcanism of Medvezhia caldera on the Iturup Island of Kurile Isles: impact of regional tectonics on subduction magmatism. *International Geology Review* 65 (2), 179–199, DOI: [10.1080/00206814.2022.2039885](https://doi.org/10.1080/00206814.2022.2039885).
- Melekeshev, I.V. (1974).** The outer ridge of the Kuril Arc, in: Luchitsky, I.V. (Ed.). *Kamchatka, Kuril and Commander Islands* [in Russian], Nauka, Moscow, pp. 265–327.
- Melekestsev, I.V., Volynets, O.N., Antonov, A.Yu. (1997).** Caldera Nemo III (Onkotan Island, Northern Kuriles): structure, <sup>14</sup>C-age, dynamics of caldera-forming eruption, evolution of juvenile products. *Volcanology and Seismology* (1), 32–51.
- Melekestsev, I.V., Braitseva, O.A., Sulerzhitskii, L.D. (1988).** Catastrophic explosive eruptions of the Kurilo-Kamchatka region in the end of Pleistocene - beginning of Holocene. *Doklady Akademii Nauk SSSR* 300 (1), 175–181.

- Melekestsev, I.V., Braitseva, O.A., Ponomareva, V.V., Sulerzhitsky L.D. (1998).** ‘Century’ of volcanic disasters in the early Holocene of the Kuril-Kamchatka region, in: Dobretsov N.L., Kovalenko V.I. (Eds.). Global changes in the natural environment [in Russian]. Publishing House, SB RAS, OIGGM, Novosibirsk, pp. 146–152.
- Milne, J. (1879).** Cruise among the Volcanos of the Kurile Islands. *Geological Magazine* 6 (8), 337–348.
- Nakagawa, M., Ishizuka, Y., Hasegawa, T., Baba, A., Kosugi, A. (2008).** Preliminary report on volcanological research of KBP 2007-08 cruise by Japanese volcanology group. Sapporo, Hokkaido University.
- Nandedkar, R.H., Ulmer, P., Müntener, O. (2014).** Fractional crystallization of primitive, hydrous arc magmas: an experimental study at 0.7 GPa. *Contributions to Mineralogy and Petrology* 167 (6), 1015, DOI: [10.1007/s00410-014-1015-5](https://doi.org/10.1007/s00410-014-1015-5).
- Newhall, C.G., Dzurisin, D. (1988).** Historical Unrest at Large Calderas of the World, V.1 & 2, US Geological Survey, Washington.
- Ostapenko, V.F., Fedorchenko, V.I., Shilov, V.N. (1967).** Pumices, ignimbrites and rhyolites from Great Kurile Arc. *Bulletin of Volcanology* 30 (1), 81–92, DOI: [10.1007/BF02597658](https://doi.org/10.1007/BF02597658).
- Ostapenko, V.F. (1970).** Morphology and structure of the Medvezhy caldera volcano (Iturup Island, Kuril), in: *Izvestiya of the Sakhalin Department of the Geographical Society of the USSR*, 1, pp. 99–108, [in Russian].
- Petford, N., Gallagher, K. (2001).** Partial melting of mafic (amphibolitic) lower crust by periodic influx of basaltic magma. *Earth and Planetary Science Letters* 193 (3–4), 483–499, DOI: [10.1016/S0012-821X\(01\)00481-2](https://doi.org/10.1016/S0012-821X(01)00481-2).
- Plekhov, P.Yu., Balashova, A.L., Dirksen, O.V. (2010).** Magma degassing during 7600 <sup>14</sup>C Kurile Lake caldera-forming eruption and its climatic effect. *Doklady Earth Sciences* 433 (1), 974–977, DOI: [10.1134/S1028334X10070275](https://doi.org/10.1134/S1028334X10070275).
- Poli, P., Shapiro, N. M. (2022).** Rapid characterization of large volcanic eruptions: measuring the impulse of the Hunga Tonga Ha’apai explosion from teleseismic waves. *Geophysical Research Letters* 49 (8), DOI: [10.1029/2022GL098123](https://doi.org/10.1029/2022GL098123).
- Ponomareva, V. V., Kyle, P. R., Melekestsev, I. V., Rinkleff, P. G., Dirksen, O. V., Sulerzhitsky, L. D., Zaretskaia, N. E., Rourke, R. (2004).** The 7600 (<sup>14</sup>C) year BP Kurile Lake caldera-forming eruption, Kamchatka, Russia: stratigraphy and field relationships. *Journal of Volcanology and Geothermal Research* 136 (3), 199–222, DOI: [10.1016/j.jvolgeores.2004.05.013](https://doi.org/10.1016/j.jvolgeores.2004.05.013).
- Ponomareva, V., Portnyagin, M., Davies, S. M. (2015).** Tephra without borders: Far-reaching clues into past explosive eruptions. *Frontiers Earth Science* 3, 83, DOI: [10.3389/feart.2015.00083](https://doi.org/10.3389/feart.2015.00083).
- Ponomareva, V. V., Portnyagin, M. V., Bubenshchikova, N. V., Zelenin, E. A., Derkachev, A. N., Jicha, B., Gorbarenko, S. A., Cook, E., Garbe-Schonberg, D., Hoernle, K. (2023).** A 6.2 Ma-long record of major explosive eruptions from the NW Pacific volcanic arcs based on the offshore tephra sequences on the northern tip of the Emperor Seamount Chain. *Geochemistry, Geophysics, Geosystems* 24 (12), DOI: [10.1029/2023GC011126](https://doi.org/10.1029/2023GC011126).
- Proshkina, Z.N., Kulinich, R.G., Valitov, M.G. (2017).** Structure, matter composition, and deep structure of the oceanic slope of the Central Kuril Island: New evidence. *Russian Journal of Pacific Geology* 11 (6), 436–446, DOI: [10.1134/S1819714017060045](https://doi.org/10.1134/S1819714017060045).
- Razzhigaeva, N.G., Matsumoto, A., Nakagawa, M. (2016).** Age, source, and distribution of Holocene tephra in the southern Kurile Islands: Evaluation of Holocene eruptive activities in the southern Kurile arc. *Quaternary International* 397, 63–78, DOI: [10.1016/j.quaint.2015.07.070](https://doi.org/10.1016/j.quaint.2015.07.070).
- Rickwood, P.C. (1989).** Boundary lines within petrologic diagrams, which use oxides of major and minor elements. *Lithos* 22 (4), 247–263, DOI: [10.1016/0024-4937\(89\)90028-5](https://doi.org/10.1016/0024-4937(89)90028-5).
- Rybin, A.V., Razzhigaeva, N.G., Guryanov, V.B., Degterev, A.V., Chibisova, M.V. (2015).** The main stages of the formation of Tyatya Volcano (Kunashir Island, Kuril Islands), in: All-Russian conference ‘Geodynamic processes and natural disasters. Experience of Neftegorsk’. Dalnauka, Vladivostok, pp. 271–273.
- Rybin, A.V., Degterev, A.V., Dudchenko, I.P., Guryanov, V.B., Romanyuk, F.A., Klimantsov, I.M. (2017).** Comprehensive research on Matua Island in 2017. *Geosystems of Transition Zones* 1 (4), 21–29, DOI: [10.30730/2541-8912.2017.1.4.021-029](https://doi.org/10.30730/2541-8912.2017.1.4.021-029).
- Shand, S.J. (1943).** Eruptive rocks: their genesis, composition, classification, and their relation to ore deposits with a chapter on meteorites. John Wiley, New York.
- Simon, J.I., Weis, D., DePaolo, D.J., Renne, P.R., Mundil, R., Schmitt, A.K. (2014).** Assimilation of preexisting Pleistocene intrusions at Long Valley by periodic magma recharge accelerates rhyolite generation: rethinking the remelting model. *Contributions to Mineralogy and Petrology* 167 (1), 955, DOI: [10.1007/s00410-013-0955-5](https://doi.org/10.1007/s00410-013-0955-5).
- Smirnov, S. Z., Rybin, A. V., Sokolova, E. N., Kuzmin, D. V., Degterev, A. V., Timina, T. Y. (2017).** Felsic magmas of the caldera-forming eruptions on the Iturup Island: the first results of studies of melt inclusions in phenocrysts from pumices of the Lvinaya Past and Vetrovoy Isthmus calderas. *Russian Journal of Pacific Geology* 11 (1), 46–63, DOI: [10.1134/S1819714017010080](https://doi.org/10.1134/S1819714017010080).
- Smirnov, S. Z., Rybin, A. V., Kruk, N. N., Timina, T. Y., Sokolova, E. N., Kuzmin, D. V., Maksimovich, I. A., Kotov, A. A., Shevko, A. Y., Nizametdinov, I. R., Abersteiner, A. (2019).** Parental melts and magma storage of a large-volume dacite eruption at Vetrovoy Isthmus (Iturup Island, Southern Kuril Islands): Insights into the genesis of subduction-zone dacites. *Journal of Petrology* 60 (7), 1349–1370, DOI: [10.1093/petrology/egz032](https://doi.org/10.1093/petrology/egz032).
- Sparks, R.S.J., Self, S., Walker, G.P.L. (1973).** Products of ignimbrite eruptions. *Geology* 1, 115–118, DOI: [10.1130/0091-7613\(1973\)1%3C](https://doi.org/10.1130/0091-7613(1973)1%3C).
- Sparks, S. R. J., Sigurdsson, H., Wilson, L. (1977).** Magma mixing a mechanism for triggering acid explosive eruptions. *Nature*, 267 (5609), 315–318, DOI: [10.1038/267315a0](https://doi.org/10.1038/267315a0).
- Stern, R.J. (2010).** The anatomy and ontogeny of modern intra-oceanic arc systems. Geological Society, London, Special Publications, 338 (1), 7–34, DOI: [10.1144/SP338.2](https://doi.org/10.1144/SP338.2).
- Vitte, L.V. (1981).** Types of continental crust and history of their evolution. Nauka, Moscow, [in Russian].
- Volynets, O.N., Ponomareva, V.V., Braitseva, O.A., Melekestsev, I.V., Chen, Ch.H. (1999).** Holocene eruptive history of Ksudach volcanic massif, South Kamchatka: evolution of a large magmatic chamber. *Journal of Volcanology and Geothermal Research*, 91 (1), 23–42, DOI: [10.1016/s0377-0273\(99\)00049-9](https://doi.org/10.1016/s0377-0273(99)00049-9).
- White, A.J.R. (1979).** Sources of granite magmas. *Geological Society of America. Abstracts with Programs*, 11, 539.
- Williams, H. (1941).** Calderas and their origin. University of California Press.
- Wilson, C.J.N., Rogan, A.M., Smith, I.E.M., Northey, D.J., Nairn, I.A., Houghton, B.F. (1984).** Caldera volcanoes of the Taupo Volcanic Zone, New Zealand. *Journal of Geophysical Research Solid Earth* 89 (B10), 8463–8484, DOI: [10.1029/JB089iB10p08463](https://doi.org/10.1029/JB089iB10p08463).
- Zlobin, T.K., Levin, B.W., Polets, A.Y. (2008).** First results of the comparison of catastrophic Simushir earthquakes on November 15, 2006 ( $M = 8.3$ ), and January 13, 2007 ( $M = 8.1$ ), with the deep structure of the Earth’s crust in the Central Kuril Islands. *Doklady Earth Sciences* 420, 615–619, DOI: [10.1134/S1028334X08040193](https://doi.org/10.1134/S1028334X08040193).